A Drell -Yan Experiment with a Transversly Polarized Target at SeaQuest
version: 0.2

E1039 Collaboration

August 1, 2016

Abstract

It is well known that the proton is a spin-1/2 particle, but how the constituents (quarks and gluons) assemble to this quantized spin is still a mystery. There is a worldwide effort to map out the individual contributions to the proton spin. It is established that the quark spins contribute around 30%, while the gluon intrinsic angular momentum is still under active investigation at the Relativistic Heavy Ion Collider . While much progress has been made during the last few decades on the heilcity distributions, which sample the amount of partons with longitudinal spin parallel or antiparallel to the spin of the parent nucleon, fully resolving the proton spin puzzle requires information on the orbital angular momentum (OAM) of both quarks and gluons. To achieve a complete understanding of the internal properties of the nucleon, necessary to resolve the sin puzzle, the study of the transverse degrees of freedom of the partons are best suited. This transverse information is encoded in eight so called Transverse Momentum Distributions (TMD). One of the most important TMDs, and the main focus of this LOI, is the so-called Sivers function. We propose to measure the Sivers function for the $\bar{u}$ and $\bar{d}$ seaquarks in the nucleon for four different Bjorken $x_B(.1 < x_B < .5)$ using the Drell-Yan process. We will use the 120 GeV Fermilab main injector proton beam with a newly commissioned, high luminosity transversely polarized proton and deuteron target together with the SeaQuest spectrometer.

Abstract

Contents

1 Tasks to be done

1. check references. Make sure xarch is replaced with real pub

2 Introduction

It is well known that the proton is a spin-1/2 particle, but how the constituents (quarks and gluons) assemble to this quantized spin is still a mystery. There is a worldwide effort to map out the individual contributions to the proton spin [1] [2]. It is established that the quark spins contribute around 30%, while the gluon intrinsic angular momentum is still under active investigation at the Relativistic Heavy Ion Collider [3]. While much progress has been made during the last few decades on the heilcity distributions, which sample the amount of partons with longitudinal spin parallel or antiparallel to the spin of the parent nucleon, fully resolving the proton spin puzzle requires information on the orbital angular momentum (OAM) of both quarks and gluons. To achieve a complete understanding of the internal properties of the nucleon, necessary to resolve the sin puzzle, the study of the transverse degrees of freedom of the partons are best suited. This transverse information is encoded in eight so called Transverse Momentum Distributions (TMD).

One of the most important TMDs, and the main focus of this proposal, is the so-called Sivers function [4]. It was introduced in 1990 to help explain the large transverse single-spin asymmetries observed in hadronic pion production at Fermilab [5]. The quark Sivers function represents the momentum distribution of unpolarized quarks inside a transversely polarized proton, through a correlation between the quark momentum transverse to the beam and the proton spin. On one hand, the Sivers function contains information on both the longitudinal and transverse motion of the partons and provides a unique way to perform 3-dimensional proton tomography in momentum space [1] [2] . On the other hand, it has been shown that there is a close connection between the Sivers function and quark OAM. Though the search for a rigorous, model-independent connection is still ongoing, it is clear that the existence of a non-zero Sivers function requires non-zero quark OAM [1]. From a detailed analysis of the azimuthal distribution of the produced particles from a transversely polarized nucleon, one can deduce properties of the nucleon structure.

This approach has been used in Semi-Inclusive Deep Inelastic Scattering (SIDIS) experiments, where non-zero values of the Sivers function from HERMES [6] COMPASS [7]and JLab [8] have indicated that the orbital angular momentum of the up quarks is positive ($L_u > 0$) but of the down quarks is negative ($L_d < 0$). The anti-down versus anti-up quark excess in the proton observed in Drell-Yan (DY) measurements by E866 1 when interpreted in the pion cloud model, provides a strong hint that the sea quarks contribute significantly to the orbital angular mo-

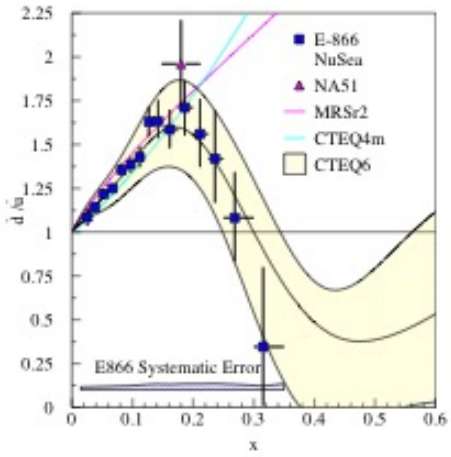

Figure 1: *E866 DY result for anti-down versus anti-up quark content of the proton. If the excess of anti-down quarks is due to a pion cloud around the proton, then the pions (and sea quarks) contribute a significant amount of orbital angular momentum.*

mentum [9], in the x range where significant valence quark Sivers asymmetries were observed in SIDIS. However, current SIDIS experiments have little sensitivity to the antiquark Sivers asymmetry in this kinematic range. Thus, a direct measurement of the Sivers function for the antiquarks has become crucial and can only be accessed cleanly via the Drell-Yan process 2. We propose to carry out the first measurement of the sea quark Sivers function, using Drell-Yan production from an unpolarized 120 GeV proton beam scattering off a transversely polarized proton target.

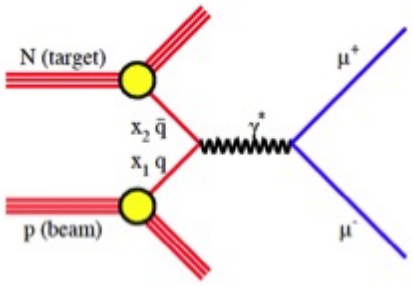

Figure 2: *A Feynman diagram for the Drell Yan process*

Additionally we will also measure the Sivers function of the d-bar quarks, thus

allowing us to determine if there is a flavor asymmetry in the Sivers function of the sea, as has been observed for the valence quarks. In that case, the orbital angular momenta of u and d valence quarks are large but opposite in sign, leading to an overall small contribution to the nucleon spin. It is therefore essential for our understanding of the sea quark angular momentum to measure both the u-bar and d-bar Sivers function. Measurements by the NMC collaboration at CERN and the LANL-led Experiment E866 at FNAL showed that the Gottfried Sum Rule, which predicted a symmetric sea quark momentum distribution, was badly violated (Figure 1). The origin of this violation of perturbative QCD is still not understood and has led to the development of many different theoretical models. As a consequence, large differences between the u-bar and d-bar Sivers asymmetry are now expected. One of the leading hypotheses, the pion cloud model of the proton, predicts a direct connection between the d-bar excess seen in E866 (Figure 2) and the orbital angular momentum of the d-bar sea. Determining which theoretical model is correct can only be achieved by measuring both the u-bar and d-bar Sivers asymmetry with Drell-Yan, which requires both a polarized proton and neutron target.

Besides helping to resolve the proton spin puzzle, this proposal helps address the recent NSAC milestone HP13 to "test unique QCD predictions for relations between single transverse spin phenomena in p-p scattering and those observed in deep inelastic lepton scattering." A fundamental prediction of QCD is that the Sivers function changes sign, when going from SIDIS to DY production [10]. This prediction is deeply rooted in the gauge structure of QCD as a field theory, and is based on the well-known QCD factorization formalism widely used in interpreting high-energy experimental data. Thus, its experimental verification or refutation is crucial. The existing SIDIS data from HERMES, COMPASS and JLab [6, 7, 8] have enabled us only to extract the Sivers function of valence quarks. This LOI proposes to make the first determination of the size and the sign of the sea quark Sivers function. Combined with higher luminosity SIDIS experiments planned at JLAB, which aim to measure the Sivers distribution for sea quarks, our results would allow a test of this fundamental prediction of QCD. Higher luminosity SIDIS experiments planned at JLAB should be able to measure the sea quark Sivers distribution for direct comparison with our results.

To summarize, we propose to make the first measurement of the Sivers function of sea quarks, which is expected to be non-zero if the sea quarks contribute orbital angular momentum to the proton spin, as expected from the pion cloud model which also partially explains the E866 results.

Specifically, we will determine the Sivers functions for both the the anti-up

and anti-d quarks, with Bjorken-x in the range of 0.1 to 0.5. Drell-Yan production off polarized proton and deuteron targets have never been measured and are complementary to the approved (stage-1) experiment E1027 at Fermilab [11] , which will measure the Sivers function of the valence quarks using a polarized proton beam on an unpolarized proton target. If the measured sea quark Sivers function is non-zero, we will also determine its sign.

Should we say anything about the fact that polarized beam together with polarized target will allow us to measure the transversity distribution in the cleanest way?

It is important to note that the proposed measurementt is the only currently planned experiment which will cleanly access the seaquark Sivers function. While SIDIS is dominated by the valence quarks and is insensitive to the sea contribution. COMPASS at CERN, using pion induced Drell-Yan probes the valence region due to the antiquark content of the beam. RHIC W is different, and also differen Q need to address this.

3 Motivation

3.1 Theory

The fundamental importance of studying transverse momentum distributions and advancing the related theory of the nucleon spin is well summarized by the goals of the nuclear theory TMD Topical Collaboration, where LANL is a key member [13].

Nucleons (protons and neutrons) are the fundamental building blocks of atomic nuclei and make up essentially all the visible matter in the universe. Our modern understanding of the strong interaction is based on Quantum Chromodynamics (QCD) and in this theory, the nucleon arises as a strongly interacting, relativistic bound state of quarks and gluons (referred to as partons). The nucleon is not static, but has complex internal structure, full of features that ultimately emerge from QCD dynamics and that are only now beginning to be revealed in modern experiments. Explaining the origin, the evolution, and the structure of the visible world is a central goal of nuclear physics. In order to do this, it is vital to understand the internal structure of the nucleon in terms of its partonic constituents.

Over the last 50 years, since the first deep inelastic scattering experiments, there have been many advances in our understanding of the partonic structure of the nucleon, including its momentum and spin structure. The most significant

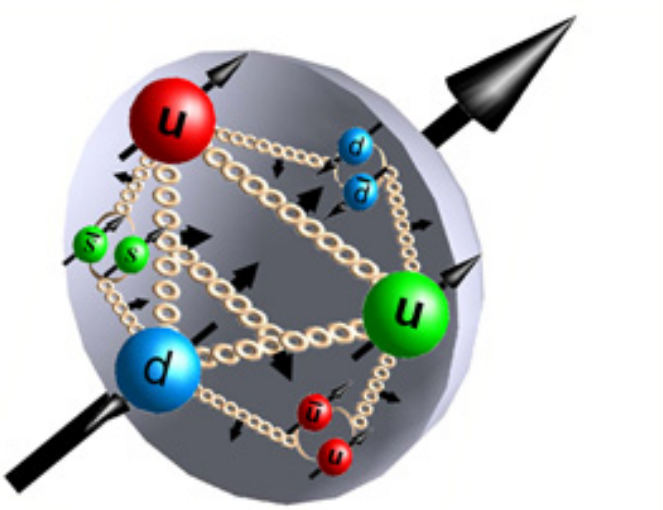

Figure 3: *Proton as a dynamical system of quarks and gluons.*

progress has been in understanding the longitudinal distribution of quarks and gluons encoded in the standard unpolarized parton distributions $f(x, Q)$. However there are still unknown aspects of the nucleon structure, especially the ones related to the transverse distribution of partons and its full 3-dimensional landscape. With the running of the COMPASS experiment at CERN, RHIC at BNL, the E906/SeaQuest Drell-Yan experiment at Fermilab, e^+e^- annihilation experiments at Belle and BaBar, and experiments at JLab, we have uncovered the first layers of transverse partonic structure of the proton. It is critical to ramp up the experimental investigation of TMDs and provide accurate and thus far missing experimental information on polarized proton reactions to enable much needed breakthroughs in QCD theory.

3.1.1 TMDs

Transverse momentum dependence in the parton distributions of the nucleon allows for the appearance of unsuppressed single spin azimuthal asymmetries, such as Sivers [4] and Collins [10] asymmetries. Fully color gauge invariant expressions for matrix elements that appear in these asymmetries can be written to leading $\mathcal{O}(1)$ [14] and subleading $\mathcal{O}(M/P^+)$ [15] powers, where M is the nucleon mass and P^+ is its large lightcone momentum. The full quark correlation function $\Phi(x, p_T)$ to $\mathcal{O}(1)$, consistent with the conditions imposed by hermiticity and

parity is given by

$$\Phi(x,\boldsymbol{p}_T) = \frac{1}{2}\Bigg\{ f_1(x,\boldsymbol{p}_T^2)\,\not{n}_+ + g_{1s}(x,\boldsymbol{p}_T)\,\gamma_5\,\not{n}_+ + h_{1T}(x,\boldsymbol{p}_T^2)\,\frac{\gamma_5\,[\not{S}_T,\not{n}_+]}{2} + h_{1s}^{\perp}(x,\boldsymbol{p}_T)\,\frac{\gamma_5\,[\not{p}_T,\not{n}_+]}{2M} + f_{1T}^{\perp}(x,\boldsymbol{p}_T^2)\,\frac{\epsilon_{\mu\nu\rho\sigma}\gamma^\mu n_+^\nu p_T^\rho S_T^\sigma}{M} + h_1^{\perp}(x,\boldsymbol{p}_T^2)\,\frac{i\,[\not{p}_T,\not{n}_+]}{2M}\Bigg\}. \quad (1)$$

Here the spin vector is defined

$$S = S_L\left(\frac{P^+}{M}\,n_+ - \frac{P^-}{M}\,n_-\right) + S_T, \quad (2)$$

and the notation

$$g_{1s}(x,\boldsymbol{p}_T) \equiv S_L\,g_{1L}(x,\boldsymbol{p}_T^2) + g_{1T}(x,\boldsymbol{p}_T^2)\,\frac{(\boldsymbol{p}_T\cdot\boldsymbol{S}_T)}{M}, \quad (3)$$

and similarly for $h_{1s}^{\perp}$, $g_s^{\perp}$ and h_s was used. The 'twist-two' distributions functions f_1, g_{1s}, h_{1T}, $h_{1s}^{\perp}$, with the longitudinal and transverse components explicitly separated where relevant, are shown in Figure 5. They represent the distribution of unpolarized, longitudinally polarized and transversely polarized quarks in unpolarized, longitudinally polarized and transversely polarized nucleons.

QUARKS	γ^+	$\gamma^+\gamma_5$	$\gamma^+\gamma^\alpha\gamma_5$
U	f_1		$h_1^\perp$
L		g_{1L}	$h_{1L}^\perp$
T	$f_{1T}^\perp$	g_{1T}	h_{1T}, $h_{1T}^\perp$

Figure 4: *Classification of the quark TMDs. Table taken from Ref. [16].*

In recent years, the study of single transverse-spin asymmetries (SSAs) has become a forefront of both experimental and theoretical research in QCD and hadron physics. With extensive experimentation underway and major theoretical advances, we have begun to obtain a deeper understanding of the nucleon structure

and the partons? Of these TMDs, the Sivers function has garnered considerable interest since it can be readily measured in semi-inclusive deep inelastic scattering experiments (SIDIS) and Drell-Yan production (DY). Defined as

$$f_1^q(x, \vec{p}_T^{\,2}) - \frac{\epsilon_T^{ij} p_T^i S_T^j}{M} f_{1T}^{\perp q}(x, \vec{p}_T^{\,2}) = \frac{1}{2}\mathrm{Tr}[\Phi^q \gamma^+] \tag{4}$$

where

$$\Phi^q(x, \vec{p}_T, S) = \int \frac{dz^- d^2\vec{z}_T}{(2\pi)^3} e^{ip^+ z^- - i\vec{p}_T \cdot \vec{z}_T} \langle P, S|\bar{\psi}^q(0)\psi^q(z)|P, S\rangle, \tag{5}$$

it is time-reversal odd (T-odd) distribution. The following questions of great experimental and theoretical significance can be answered by measuring the Sivers function in with E1039 in polarized DY reactions.

- What is the magnitude and sign of the sea quark Sivers function and how does it compare to the sign and magnitude in the valance quark region? Current SIDIS experiments allow for the accurate extraction of the Sivers function in the valence quark region. At smaller Bjorken x, where sea quarks dominate, the uncertainty in global fitting becomes large. The lack of experimental data forces fits to zero and the systematic uncertainties cannot be properly evaluated. See for example Figure 5.

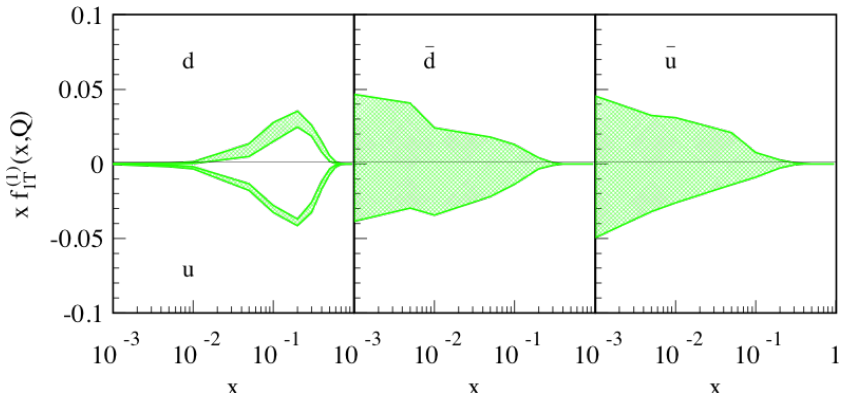

Figure 5: *Example of extraction of quark TMDs via global fitting from Ref. [17]. Shown is the collinear Qiu-Sterman function, related to the first p_T^2 moment of the quark Sivers TMD. Note the relatively small error band for valence quarks and the large error band for sea quarks.*

- What is the relation of the Sivers asymmetry measured in semi-inclusive deep inelastic scattering to the one measured in the Drell-Yan process? It is a fundamental prediction of QCD that the Sivers function should change sign in going form SIDIS to DY.

$$f_{1T}^{\perp q\ \mathrm{DY}}(x, \bar{p}_T^2) = -f_{1T}^{\perp q\ \mathrm{SIDIS}}(x, \bar{p}_T^2) \tag{6}$$

Future measurements at the electron ion collider (EIC) will help determine the sea quark Sivers function in SIDIS. The E1039 experiment will provide unique information in the sea quark Sivers function in DY that will help validate and advance QCD theory of TMDs. Even with input from relatively recent analysis of the Sivers asymmetry in SIDIS [17], the sign of the sign of the asymmetry in DY cannot be determined. This is shown in Figure 6 and in the kinematic setup we use E1039 measurements are in the region $x_F \in (-0.6, -0.2)$ with largest uncertainty.

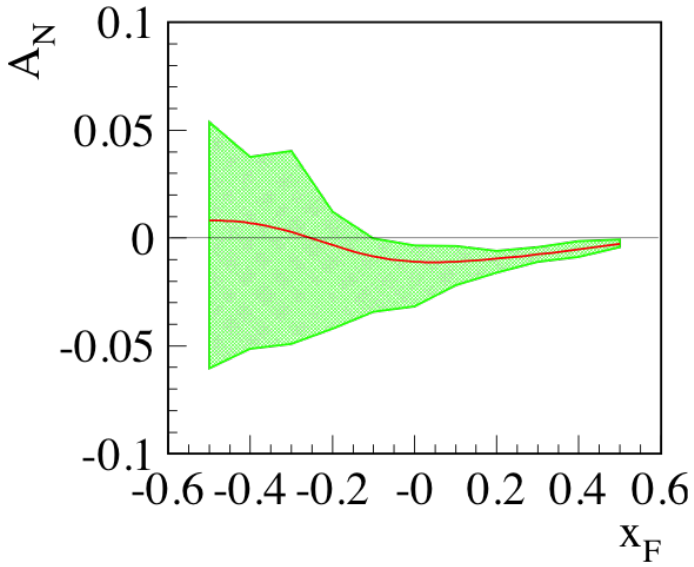

Figure 6: *Uncertainties in the predicted Sivers asymmetry in polarized Drell-Yan reactions. In this figure at Fermilab E1039 acceptance is for Feynman x -0.6 to 0.2.*

- What is the evolution of the TMDs? Quantum Chromo Dynamics provides very powerful predictions concerning the dependence (evolution) of underlying parton distribution functions on the hard scale Q of the physical

process. QCD factorization theorems separate the measured cross sections into the perturbatively calculable hard parts that encode the short distance QCD dynamics and the parton distribution and/or fragmentation functions that encode non-perturbartive long distance parton dynamics. The Transverse Momentum Dependent factorization is applicable to description of a differential cross section dependent on an additional measured scale Q_T, which allows distributions to be sensitive to the intrinsic transverse motion of quarks and gluons. TMD factorization analogously separates a differential cross section into a hard part and several well-defined universal factors [18, 19, 20]. These factors can be interpreted in terms of three-dimensional nucleon structure: they are called Transverse Momentum Dependent distribution and fragmentation functions (TMDs).

In recent decades this formalism has been improved greatly using various approaches, see Refs. [21, 22, 23, 24]. A distinct feature of the TMD evolution is dependence on the non-perturbative aspects of gluon radiation. The presence of the non perturbative functions in the mere formulation of the evolution is a great advantage and challenge of the formalism. It allows one to study details of the non perturative gluon radiation and at the same time it allows a substantial sensitivity of results to the corresponding non perturbative functions. That is, even though evolution equations are formally the same, the solutions can vary greatly depending on the choice of the non perturbative input. Implementing the formalism requires the non-perturbative inputs [25, 26, 27, 17] for the TMDs.

To understand the evolution of TMDs, it is essential to have experimental measurements at multiple scales. SIDIS measurements probe the low $Q^2 \sim$ few GeV^2 and $Q_T < 1$ GeV region (the second very important scale for TMDs). W/Z production probes the very high $Q^2 \sim 100^2$ GeV^2 and $Q_T \sim$ tens GeV region. Drell-Yan measurements above the J/ψ peak fall in a unique Q^2 region and $Q_T \sim$ few GeV and E1039 results are critical to constrain the evolution of TMDs, which is not yet well understood.

3.1.2 Orbital Angular Momentum

There is compelling experimental evidence that the sum of the quark and gluon intrinsic angular momenta only contributes $\sim 1/3$ of the total proton spin. Thus, the majority of the proton spin is unaccounted for, which has been referred to as the "proton spin crisis" [**?**]. The missing fraction of the spin is likely carried by

the orbital angular momentum of the quarks and gluons.

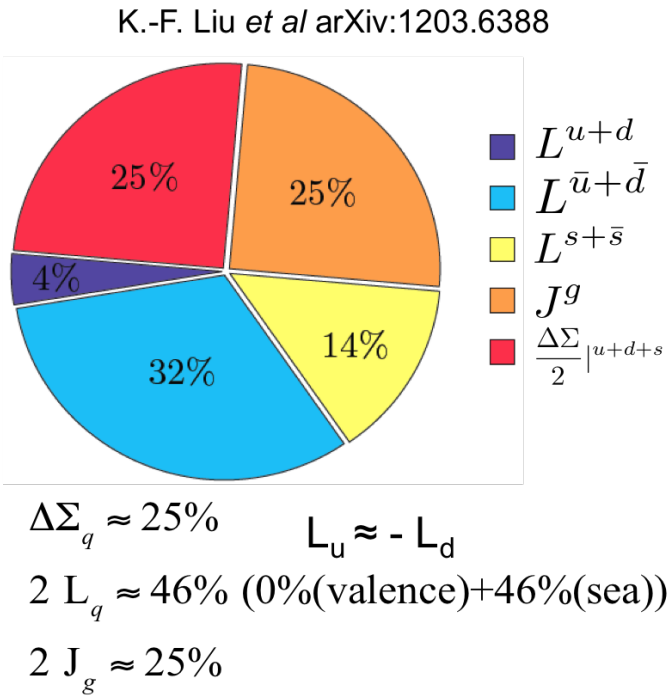

Figure 7: *Various contributions to the orbital angular momentum of nucleons as given by a calculation of K.F. Liu et al. [30].*

Recent theoretical developments have provided important insight into decomposition of the nucleon spin into its quark and gluon contributions and further separation of these into spin and orbital components [28]. One such decomposition given by Ji [29] is

$$\frac{1}{2} = S_q + L_q + J_g \ , \tag{7}$$

At present, there is no established relation between forward TMDs and the quark orbital angular momentum. It is, however, known that if the Sivers functions vanishes, $L_q = 0$.

One promising way forward is to use lattice QCD calculations to evaluate the contribution to the nucleon spin. One such calculation is shown if Figure 7, where the orbital angular momentum is carried by sea quarks [30]. The contributions form valence quarks come with opposite sign and cancel each other. This is similar to the sign difference of Sivers function for u and d quarks found from global

extractions, see for example Figure 5. Phenomenologically one can establish a relation between the strength of the Sivers functions and lattice QCD results and use this relation as a guidance to assess the sea quark contribution to the OAM.

3.2 Current theoretical and experimental status

Semi-Inclusive Deep Inelastic Scattering (SIDIS) experiments at HERMES [6] COMPASS [7]and JLab [8] have observed non-zero values of the Sivers function which indicate that the orbital angular momentum of the up quarks is positive ($L_u > 0$) but of the down quarks is negative ($L_d < 0$) Due to this cancellation, the valence quarks carry little net orbital angular momentum. This result is confirmed by Lattice QCD calculations [ref]. Echevarria, et. al. [ref], have performed a global fit of the Sivers data from SIDIS. They found that while the valence quark Sivers function are well constrained and opposite for u and d quarks, those for the sea quarks are largely unconstrained.

Further insight into the orbital angular momentum contribution for the sea quarks requires the use of two body reactions with an antiquark in the initial state. These include the Drell-Yan reaction and production of W and Z bosons. Due to their large masses, the W and Z measurements are only feasible at high energy collider facilities. Small asymmetries cannot usually be observed, due to limited statistics. The STAR experiment at RHIC has published transverse single spin asymmetries for W's [ref]. While the statistics are quite limited, the asymmetries appear to be non-zero and positive for both W^+ and W^-. STAR may collect additional data in the future, but the measurement will always hampered by the small cross section for W's. Drell-Yan production in fixed target experiments is much more promising, as the integrated luminosity can be much larger. The COMPASS experiment at CERN and the ANDY experiment at RHIC have performed transverse single spin asymmetry measurements. COMPASS used a secondary pion beam. Due to the presence of the antiquark in the pion, COMPASS is primarily sensitive to valence quarks in the polarized target. ANDY was unable to acquire sufficient statistics to observe a meaningful asymmetry.

Thus, no existing experiment is capable of measuring the Sivers asymmetry of the sea quarks. Our proposed E1039 experiment at Fermilab has all of the required performance metrics. E1039 is based upon the proven E906 spectrometer, which has already acquired large numbers (?) of Drell-Yan events from liquid hydrogen and deuterium targets, being primarily sensitive to the antiquark sea. LANL and UVa have recently completed and tested a new transversely polarized proton target capable of both high polarization and integrated luminosity. We note that the

proposed E1027 experiment at FNAL would instead use a transversely polarized beam with the E906 experiment to measure the valence quark Sivers function, similar to COMPASS. Another unique capability of E1039 is the ability to separately measure the Sivers function for the $\bar{d}$ and $\bar{u}$ quarks using polarized NH_3 and ND_3 targets, thus allowing us to determine if there is a flavor asymmetry in the orbital angular momentum of the sea, as has been observed for the unpolarized sea. It is therefore essential for our understanding of the sea quark angular momentum to measure both the $\bar{d}$ and $\bar{u}$ Sivers function.

There are a few theoretical estimates available for the magnitude of the Sivers asymmetry in Drell-Yan, based on global fits to the existing SIDIS data. Anselmino, et. al. [ref] and Sun and Yuan [ref] predict central Sivers values ranging from 0. to 0.2 but have very large uncertainty bands, as shown in Figure xx. More recently, Echevarria, et. al. [ref], predict asymmetries at the few % level, but note that the fits to the existing data are rather insensitive to contributions from the anti-quarks. Lattice QCD calculations predict a large net orbital angular momentum contribution from the sea quarks[ref].

At present, there is no direct theoretical relation between the Sivers function and the orbital angular momentum of the quarks. What is known is that the sign of the Sivers function should be opposite for Drell-Yan versus SIDIS and that a non zero Sivers function implies non-zero orbital angular momentum. However, there is a large ongoing theoretical effort to address this problem. Theory takes over here.....

3.3 The Drell Yan Process

The Drell-Yan process [12] describes the hadron-hadron collisisions, where a quark from one particle annihilates with an antiquark from the other particle into a virtual gamma. The gamma subsequently decays into two leptons, ℓ^+ and ℓ^-. This process is schematically shown in the Feynman diagram in Fig.2. In our proposed experiment we will use $p+ p^{\uparrow}$and $p+ d^{\uparrow}$, while COMPASS uses $\pi+ p^{\uparrow}$. To lowest order, the cross section for the Drell Yan process depends on the product of the quark and antiquark distributions $q, \bar{q}$in the beam $x_1$and in the target x_2, where x_1,$x_2$are the Bjorken x and express the fraction of the longitudinal momentum of the hadron carried by the quark.

$$\frac{d\sigma}{dx_1 dx_2} = \frac{4\pi\alpha^2}{9sx_1x_2} \sum_i e_i^2 (q_i^T(x_1, Q^2)\bar{q}_i^B(x_2, Q^2) + \bar{q}_i^T(x_1, Q^2)q_i^B(x_2, Q^2) \quad (8)$$

s is the square of the center of mass energy and is given by $s = 2m_T * E_{Beam} + m_T^2 + m_B^2$ with E_{Beam} the beam energy and the $m_{B,T}$ the rest masses of the beam and target particles. Measuring the two decay leptons in the spectrometer allows one then to determine the photon center of mass momentum $p_{\|}^{\gamma}$ (longitudinal) and p_T^{γ} (transverse) as well as the mass M_{γ}. From these quantities one can then deduce the momentum fractions of the quarks through:

$$x_F = \frac{p_{\|}^{\gamma}}{p_{\|}^{\gamma,max}} = x_1 - x_2 \tag{9}$$

$$x_1 x_2 = M_{\gamma}^2 \tag{10}$$

If one chooses the kinematics of the experiment such that $x_F > 0$ and $x_1$large , the contributions from the valence quarks in the beam dominate.

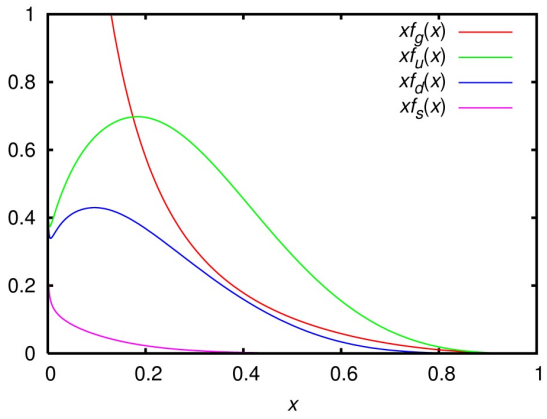

Figure 8: *The CTEQ6 parton distributions*

In this case , in equation 8 the second term becomes negligible and the cross section can be written as

$$\frac{d\sigma}{dx_1 dx_2} \approx \frac{4\pi\alpha^2}{9sx_1x_2} \sum_i e_i^2 q_i^T(x_1, Q^2) \bar{q}_i^B(x_2, Q^2) \tag{11}$$

In the case of a proton beam on a proton target the process is dominated by the $u(x_1)$ distribution due to the charge factor e_i^2. To extract the $d(\bar{x})$Sivers function one has to measure $p + d$. In the following discussion we will assume that the deuteron cross section is the sum of the proton and neutron cross section and use charge symmetry to equate $\bar{d}_p$ and $\bar{u}_n$. Ignoring strange and heavier antiquarks

in the target as well as antiquarks in the beam we can write ($x_1 >> x_2$): we can write:

$$\sigma^{pp} \propto \frac{4}{9} u(x_1)\bar{u}(x_2) + \frac{1}{9} d(x_1)\bar{d}(x_2) \tag{12}$$

$$\sigma^{pn} \propto \frac{4}{9} u(x_1)\bar{d}(x_2) + \frac{1}{9} d(x_1)\bar{u}(x_2) \tag{13}$$

$$\left.\frac{\sigma^{pd}}{2\sigma^{pp}}\right|_{x_1>>x_2} \approx \frac{1}{2} \frac{\left(1+\frac{d(x_1)}{4u(x_1)}\right)}{\left(1+\frac{d(x_1)\bar{d}(x_2)}{4u(x_1)\bar{u}(x_2)}\right)} \left(1+\frac{\bar{d}(x_2)}{\bar{u}(x_2}\right) \approx \frac{1}{2}\left(1+\frac{\bar{d}(x_2)}{\bar{u}(x_2}\right) \tag{14}$$

Therefore, through a simultaneous measurement of the pp and pd asymmetries one can independently extract the Sivers functions for both $\bar{u}$ and $\bar{d}$. Having three independent cells on a target stick, we can fill one of them with NH_3 and two with ND_3 to minimize systematic errors between the two measurements.

4 Experimental Setup and spectrometer

We are proposing to use the existing E906/SeaQuest Fig.**??** spectrometer to perform our measurement. The spectrometer consists of two magnets, FMAG and KMAG ,and four tracking stations, where the last one serves as a muon identifier. It was designed to perform Drell-Yan measurements at large x_1. This is illustrated in Fig. **??**, where the acceptance of SeaQuest is plotted as function of x_1(xaxis) and x_2(yaxis).

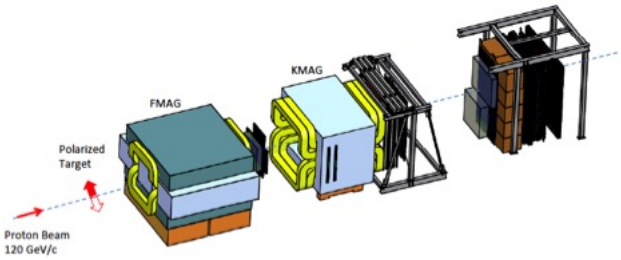

Figure 9: *The SeaQuest Spectrometer*

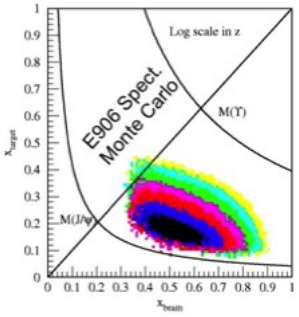

Figure 10: *The Seaquest Acceptance*

This is an excellent kinematic range for the proposed sea quark Sivers function measurement, covering the region of large anti-down quark excess observed by

E866, where large pion-cloud effects may be expected. The contributions from target valence quarks at large $x_2$are then negligible as can be seen from figure 8.

The experiment will be using the Fermilab main injector beam with an energy of 120 GeV and a 5 second spill every minute. The maximum beam intensity will be 10^{13} protons per spill.

4.1 The Polarized Target

We will use the LANL-UVa polarized target which has been built and tested over the last three years. The target system consists of a 5T superconducting split coil, a He^4 evaporation refrigerator, a 140 GHz microwave tube and a large 15'000 m^3/hr pumping system. The target is polarized using Dynamic Nuclear Polarization (DNP) [32] and is shown schematically in Figure 11. The beam direction is from left to right, and the field direction is vertical along the symmetry axis, so that the target polarization is transverse to the beam direction. In gold color the target cells are shown, with the top cell in the center of the split coils.The full system is shown in the figure 12.

While the magnetic moment of the proton is too small to lead to a sizable polarization in a 5 T field through the Zeeman effect, electrons in that field at 1 K are better than 99% polarized. By doping a suitable solid target material with paramagnetic radicals to provide unpaired electron spins, one can make use of the highly polarized state of the electrons. The dipole-dipole interaction between the nucleon and the electron leads to hyperfine splitting, providing the coupling between the two spin species. By applying a suitable microwave signal, one can populate the desired spin states. We will use frozen ammonia (NH_3 and ND_3) as the target material and create the paramagnetic radicals (roughly 10^{19} spins/ml) through irradiation with a high intensity electron beam at NIST. The cryogenic refrigerator, which works on the principle of liquid 4He evaporation can cool the bath to 1 K, by lowering the 4He vapor pressure down to $<$0.118 Torr. The polarization will be measured with NMR techniques. with three NMR coils per cell, placed inside the target. The maximum polarization achieved with the proton target is better than 92% and the ammonia bead packing fraction is about 60%. In our estimate for the statistical precision, we have assumed an average polarization of 80%. In the case of the deuterium target we have assume 30% polarization for the average.The polarization dilution factor, which is the ratio of free polarized protons to the total number of nucleons, is 3/17 for NH_3 and 3/10 for ND_3, due to the presence of nitrogen. The target material will need to be replaced approximately every 5 -8 days, due to the beam induced radiation damage. This work

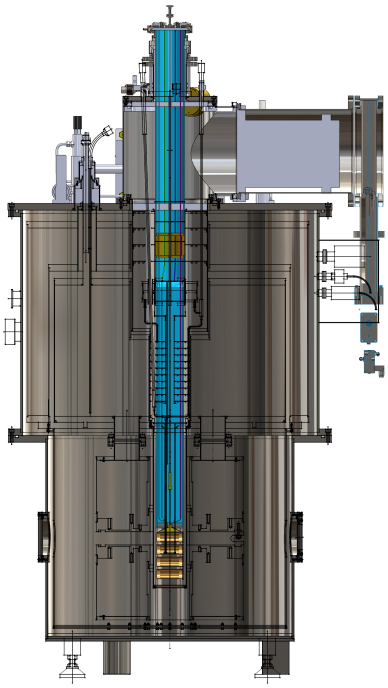

Figure 11: *A schematic representation of a split coil polarized target system*

Figure 12: *The LANL-UVa target*

will involve replacing the target stick with a new insert, cooling down the target and performing a thermal equilibrium measurement. From previous experience, we estimate that this will take about a shift to accomplish. Careful planning of these changes will reduce the impact on the beam time. Furthermore, we will be running with three active targets on one stick, thus reducing any additional loss of beam time. The target cells are 79 mm long and elliptical with 21 mm x 19mm as vertical and horizontal axes. Each cell contains 3 NMR coils spaced evenly over the whole length.

Material	Dens.	Dilution Factor	Packing Frac	<Pol>	Inter. Length
NH_3	.867 g/cm^3	.176	.60	80%	5.4 %
ND_3	1.007 g/cm^3	.333	.60	30%	5.4%

Table 1: *Parameters for the polarized target*

5 The current accomplishments from the LDRD

In 2013 LANL has awarded an internal grant jointly to Physics and Theory divisions to build a polarized target f and provide theoretical guidance for this experiment. This grant has provided 5 M$ for labor and equipment over three years.

5.1 Experimental

This internal grant allowed LANL and UVa to convert an old longitudinally polarized target into a transverse one and refurbished the refrigerator shown in Fig. 12. In addition, LANL's funds have been used to buy the necessary additional equipment, like the ROOTS pump system, microwave tube and power supply and develop a new NMR system to measure the polarization. This system is based on the Liverpool Q-meter design [37], but with new components, which allow a much more compact system. The new NMR is VME based and one crate will house the electronics for all nine NMR coils in use in our target system (3 cells per stick). This new system is shown in Fig 13

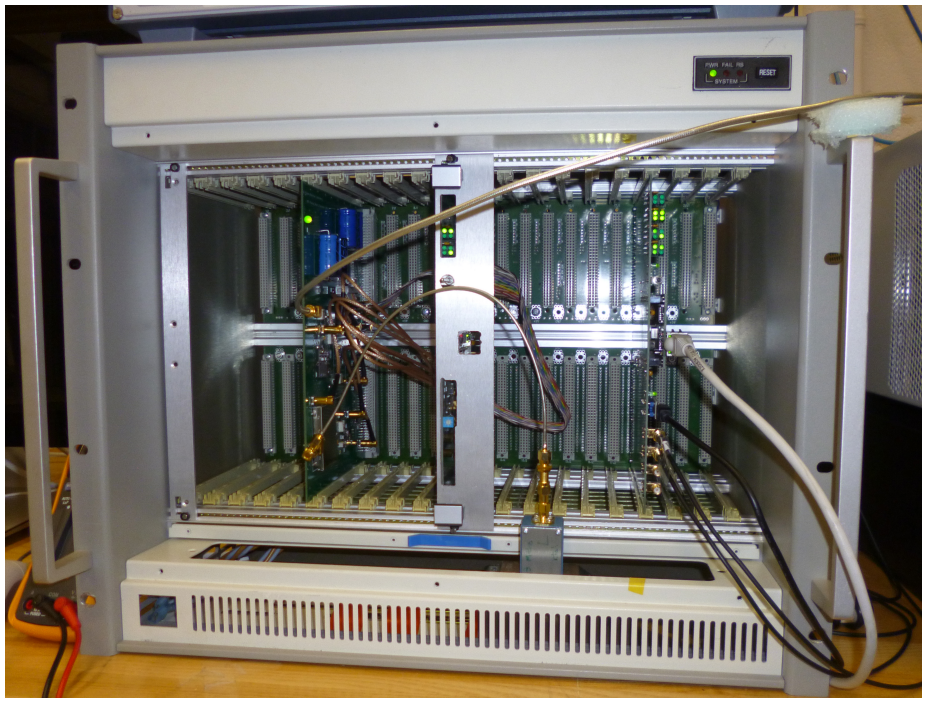

Figure 13: *The new LANL VME based NMR readout.*

To summarize, LANL's investment has allowed us to build the world's highest luminosity transversely polarized target.

5.2 Theoretical

Extracting the spin structure of the nucleon from the measurements of the quark Sivers asymmetry requires self-consistent and detailed theoretical interpretation of the Drell-Yan experiment and that measured in semi-inclusive deep inelastic lepton-proton scattering. The LDRD DR grant allowed us to initiate an integrated theory effort with three complementary components – perturbative QCD calculations, Soft Collinear Effective theory, and lattice gauge QCD. The ultimate goal is a much-improved description of the dynamical internal landscape of the nucleon from measurements of the Sivers asymmetry. The perturbative QCD effort has resulted in next-to-leading order calculations of the Sievers asymmetry in SIDIS and Drell-Yan and an extraction of Sivers function with next-to-leading logarithmic accuracy. Model calculations of quasi-parton distribution functions were also performed. The Soft Collinear Effective Theory effort has demonstrated the equivalence of the pQCD and SCET resummation approaches and calculated two-loop soft functions for use in a variety of processes. Lattice QCD has produced new results for the moments of the Sivers asymmetry from connected diagrams and compared to results from global fitting. A new method for the evaluation of disconnected diagrams has also been investigated. The integrated theory model, with its pQCD, SCET and LQCD components, was the stepping stone for the formation of the TMD Topical Collaboration in nuclear theory.

6 Integration of the Polarized Target into the SeaQuest Spectrometer

Integrating the polarized target will require some changes to the original SeaQuest setup. The location of the polarized target will be roughly 200 cm upstream from the current E906 target location. This location has been chosen to reach lower $x_2$as well as a better separation of events from the dump and the target. Furthermore, the present target cave ceiling is too low to allow for the necessary target stick changes every two weeks during the run. Preliminary MARS calculations [36] done at FNAL show that there exist some weaknesses in the shielding in NM3 which have to be addressed. In addition the shielding around FMAG has to be

partially removed and restacked to install the polarized target as well as to allow for the needed higher ceiling clearance for the target stick changes.

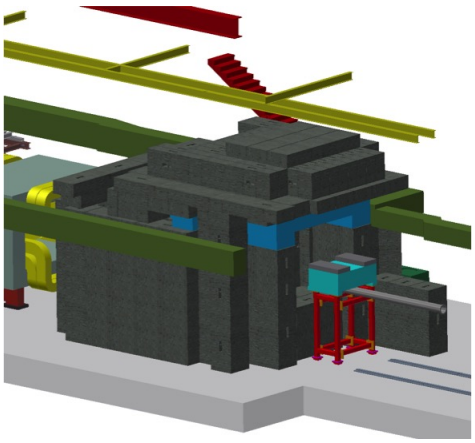

Figure 14: *The current E906 target cave and shielding*

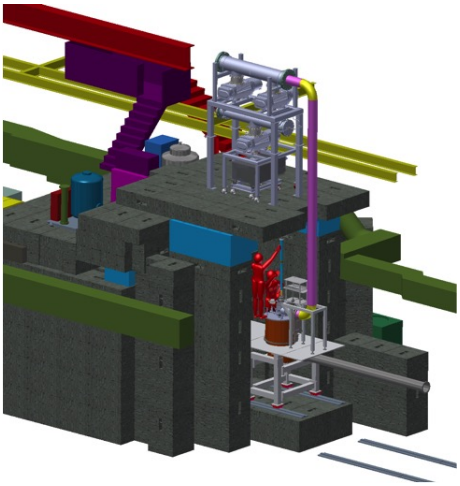

Figure 15: *The modified target cave area for E1039*

Fig 15 shows the new target area configuration, with all the additional equipment in place. While the lower part of the shielding around FMAG is the same for both configuration, one can see that E1039 requires more top clearance and therefore new shielding stacking.

The installation of the target will also necessitate some changes to the beam line. In order not to locally depolarize the target material, we require a beam spot with a "flat top" profile with minimal tails, since beam rastering is not an option. The current beam line design calls for two collimators with a dipole in between. The first collimator will shape the beam, while the dipole in conjunction with the second collimator will eliminate the created halo and tails. These collimators will also prevent the beam from accidentally hitting the superconducting coils which would result in a magnet quench.

An important part of the polarized target setup is the large ROOTS pump package, which is used to achieve the 1 K temperature in the target cell. This pump system has to be placed on top of the FMAG shielding due to space, irradiation and crane limitations in the target area. This setup will necessitate shielding penetrations for the pump lines as shown in Figure 15. Currently, we are working to determine the best locations for these penetrations, which will minimize the length of the pump lines, and at the same time fulfill the Fermilab radiation shielding re-

quirements.

Due to the fact that Helium is a non-renewable resource, we are planning to install a closed loop refrigeration liquid Helium system. The main components for this system (compressor , liquefier and storage dewars) will also be installed on top of the FMAG shielding (shown in blue and magenta on Fig. 15) , while the capture balloon for the Helium gas will be mounted to the side along the wall. The Helium and liquid Nitrogen fill lines for the system will be routed through the same shielding penetrations as the pumping lines.

6.1 The Measurements

The LANL polarized target can accomodate a variety of dynamically polarized solid targets. For the purpose of the proposed measurements, one wishes to separately measure the Sivers function for $\bar{u}$ and $\bar{d}$ quarks. The approach we will follow is similar to that used previously by experimenst E866 and E906 to measure the $\bar{d}/\bar{u}$ ratio in the proton. A transversely polarized proton target is necessary for the $\bar{u}$ Sivers measurement, where the dominant Drell-Yan channel is a valence u quark from the unpolarized proton beam annihilating with a $\bar{u}$ (sea) quark from the target to form the virtual photon. A transversely polarized deuteron target is used for the $\bar{d}$ Sivers measurement, with the neutron providing additional $\bar{d}$ (sea) quarks that annihilate with valence d quarks from the beam.

A simultaneous measurement of the Sivers function for gluons is also possible with the polarized proton target. Production of the J/ψ meson (a charmonium state) at small x_F is primarily due to gluon-gluon fusion. The J/ψ cross section and dimuon decay branch are large plus the mass of 3.097 GeV places it well within the experimental acceptance. This gluon Sivers measurement requires no hardware changes to the experiment and is discussed further in Appendix I.

6.1.1 $p + p^{\uparrow}$

A dynamically polarized NH_3 target is the optimum choice for a transversely polarized proton target. While the dilution factor is small (0.18), due to the presence of a nitrogen atom, large polarization values of up to 90% for the protons can be obtained. Measurement of Drell-Yan events at forward rapidity (positive x_F) naturally selects u(beam) + $\bar{u}$(target) with only a small a background from other quark combinations. The Sivers asymmetry is constructed from the normalized difference of the cross sections for events with opposite target polarization. Most of the systematic errors can be canceled by reversing the target polarization or the

magnetic fields of the spectrometer. The expected statistical error for a 6 month NH_3 measurement is 1% for the central x_F bins, while the systematic error is 2%.

6.1.2 $p + d^{\uparrow}$

ND_3 can used to provide the transversely polarized deuteron target. Here the dilution factor is better (0.3), but the average polarization is only about 30%, leading to similar sensitivity as for the NH_3 target. As before, statistical errors will be the dominant error in the asymmetry. A possible alternative is ^6LiD, which has an even better dilution factor (0.5). As for the proton target, events at forward rapidity select primarily sea quarks. The additional neutron in the deuteron increases the fraction of events due to d(beam) + $\bar{d}$(target). The Sivers $\bar{d}$ asymmetry is extracted from a comparison of the proton and deuteron asymmetries, using equation 5. The expected statistical error for a 6 month ND_3 measurement is 3% for the central x_F bins, with a systematic error of 2%. Use of ND_3 requires some changes to our existing polarized target. The Larmor (spin flip) frequency for deuterium is much lower than for hydrogen, 32 MHz versus 213 MHz, respectively, requiring modification of the NMR system used to measure the polarization.

Since the deuteron is a spin 1 nucleus, both vector and tensor polarizations are available. Thus, a measurement of the tensor structure function $b1$ is possible. Tensor polarization is discussed further in AppendixA.1.

7 Experimental Discussion

In the following sections, we will discuss the expected count rates and statistical precision we will achieve as well as the contributions to the systematic errors with an estimate of the dominant terms.

7.1 Count Rates and Statistical Errors

The total Drell-Yan count rates on different targets are calculated using both full GEANT4 based Monte Carlo simulation program with Drell-Yan signal events generated by the NLO calculations done by Vitev, et. al., and the demonstrated performance of Fermilab Main Inject as well as the E906/SeaQuest spectrometer.

Unlike E906/SeaQuest, the primary physics interest of E1039 experiment is to measure the low-x_2 range of polarized Drell-Yan production. We optimized

our target position from -130 cm to -300 cm, which nicely improves the low-x_2 acceptance, the triggering capability, as well as the offline target/dump separation power.

One primary bottleneck of the data collection efficiency at E906/SeaQuest is the slow Data Acquisition System (DAQ). A very tight trigger level selection has been implemented in E906/SeaQuest so as to accomodate as many events in our limited DAQ bandwidth as possible. In the summer shutdown between Run-IV (FY-2016) and Run-V (FY-2017), we will be upgrading our DAQ system to increase the bandwidth by a factor of 10, which will be avaiable for the last run of E906/SeaQuest and following experiments.

Another limiting factor of the data collection efficiency at E906/SeaQuest is the unstable instantaneous beam intensity, which is sometimes more than one order of magnitude larger than average. To prevent the spectrometer from being completely saturated, the total number of protons delivered to the target has to be limited to be less than 6×10^{12} per spill. And the data taking has to be inhibited on all neighbouring RF buckets when a high intensity bucket arrives. After careful optimization, E906/SeaQuest has been able to record on average 2.67×10^{12} protons per spill, which corresponds to 1.4×10^{18} protons per calender year.

After running for 2 years with beam time evenly split on $\mathrm{NH_3}$ and $\mathrm{ND_3}$ targets (as shown in Table 2), the integrated luminosity on $\mathrm{NH_3}(\mathrm{ND_3})$ target is expected to be $3.48 \times 10^{42}(3.70 \times 10^{42})$ cm^2. With various efficiencies assumed in Table 3, the final event yield and statistical precision of A_N measurement in each $x_2$bin is summarized in Table 4. Here the statistical precision is calculated by $\Delta A_N = \frac{1}{f}\frac{1}{P}\frac{2}{\sqrt{N}}$, where f denotes the dilution factor, P denotes the average polarization, and N denotes the event yield in each x_2 bin.

Material	Dens. (g/cm^3)	Length (cm)	Interaction Length (cm)	Dilution Factor	Packing Factor	$< P_z >$	$< P_{zz} >$
NH_3	0.917	7.9	73.5	0.176	0.6	80%	N/A
ND_3	0.987	7.9	60.1	0.3	0.6	45%	20%

Table 2: Parameters for the polarized target

Sources	Target/Acclerator	Spectrometer	Acceptance	Trigger	Reconstruction
Efficiency (%)	50	80	2.2	90	60

Table 3: Various efficiencies assumed in count rate calculation

x_2 bin	$< x_2 >$	NH_3		ND_3	
		N	ΔA (%)	N	ΔA (%)
0.10 - 0.16	0.139	0.96×10^5	4.6	1.02×10^5	4.6
0.16 - 0.19	0.175	0.86×10^5	4.8	0.91×10^5	4.9
0.19 - 0.24	0.213	1.10×10^5	4.3	1.16×10^5	4.3
0.24 - 0.60	0.295	1.05×10^5	4.4	1.12×10^5	4.4

Table 4: Event yield and statistical precision of A_N measurement in each x_2 bin on NH_3 and ND_3 targets.

7.2 Polarization Measurements

7.2.1 Proton Polarization Measurements

The nuclear spin polarization is measured with a continuous-wave NMR coil and Liverpool Q-meter [31]. The Q-meter works as part of a circuit with phase sensitivity designed to respond to the change of the impedance in the NMR coil. The radiofrequent (RF) susceptibility of the material is inductively coupled to the NMR coil which is part of a series LCR circuit, tuned to the Larmor frequency of the nuclei being probed. The output, consisting of a DC level subtracted by a post Q-meter conditioning card (Yale gain card), is then digitized and recorded as a target event [32].

this has to be rewritten for the new LANL system The polarized target NMR and data acquisition included the software control system, the Rohde & Schwarz RF generator (R&S), the Q-meter enclosure, and the target cavity insert. The Q-meter enclosure contains two separate Q-meters and Yale gain cards which are used for different target cup cells during the experiment. The target material and NMR coil are held in polychlorotrifluorethylene (Kel-F) cells with the whole target insert cryogenically cooled to 1 K. Kel-F is used because it contains no free protons.

The R&S generator produces a RF signal which is frequency modulated to sweep over the frequency range of interest. Typically, the R&S responds to an external modulation, sweeping linearly from 400 kHz below to 400 kHz above the Larmor frequency. The signal from the R&S is connected to the NMR coils within the target material. To avoid degrading reflections in the long connection from the NMR coil to the electronics, a standing wave can be created in the transmission cable by selecting a length of cable that is an integer multiple of the half-wavelength of the resonant frequency. This specialized connection cable is known as the $\lambda/2$ cable and is a semi-rigid cable with a teflon dielectric. The

NMR coil contains a single loop made of 70/30 copper-nickel tube, which minimizes interaction with the electron beam. The NMR loop opens up into an oval shape spanning approximately 2 cm inside the 2.4 cm diameter cup. The loop is located about halfway down in the center of the cup. It is possible to enhance signal to noise information through the software control system by making multiple frequency sweeps and averaging the signals. A completion of the set number of sweeps results in a single target event with a time stamp. The averaged signal is integrated to obtain a NMR polarization area for that event. Each target event written contains all NMR system parameters and the target environment variables needed to calculate the final polarization. The on-line target data and conditions are analyzed over the experiments set of target events to return a final polarization and associated uncertainty for each run.

A target NMR calibration measurement or Thermal Equilibrium measurement (TE) is used to find a proportionality relation to determine the enhanced polarization under a range of thermal conditions given the area of the "Q-curve" NMR signal at the same magnetic field. The magnetic moment in the external field results in a set of $2J$+1 energy sublevels through Zeeman interaction, where J is the particle spin. The TE natural polarization for a spin-1/2 particle is given by,

$$P_{TE} = \tanh\left(\frac{\mu B}{kT}\right), \tag{15}$$

coming from Curie's Law [**?**], where μ is the magnetic moment in the external field of strength B, k is the Boltzmann constant, and T the temperature. Measuring P_{TE} at low temperature increases stability and the polarization signal. This is favorable being that the uncertainty in the NMR signal increases as the area of the signal decreases. In fact much of the target uncertainty comes from error in the calibration.

The dynamic polarization value is derived by comparing the enhanced signal S_E integrated over the driving frequency ω, with that of the (TE) signal:

$$P_E = G\frac{\int S_E(\omega)d\omega}{\int S_{TE}(\omega)d\omega}P_{TE} = GC_{TE}A_E, \tag{16}$$

and calibration constant defined as,

$$C_{TE} = \frac{P_{TE}}{A_{TE}}. \tag{17}$$

where P_E (A_E) is the polarization (area) of the enhanced signal and P_{TE} (A_{TE}) is the polarization (area) from the thermal equilibrium measurement. The uncertainty in the calibration constant, $\delta C_{TE}/C_{TE}$, can easily be calculated using the

fractional error from P_{TE} and A_{TE}. The ratio of gains from the Yale card used during the thermal equilibrium measurement to the enhanced signal is represented as G. For more detail see, [33].

7.2.2 Neutron Polarization Measurements

The deuteron polarization will be monitored online by continuous wave NMR, using the new NMR system recently developed at LANL. There are two means whereby the polarization can be extracted from the NMR signal: the area method and the peak-height method. We intend to use both.

First, the total area of the NMR absorption signal is proportional to the vector polarization of the sample, and the constant of proportionality can be calibrated against the polarization of the sample measured under thermal equilibrium (TE) conditions. This is the standard method used for polarized proton targets, but can be more problematic for deuteron targets. Typical conditions for the TE measurements are 5 T and 1.4 K, where the deuteron polarization is only 0.075%, compared to 0.36% for protons. This smaller polarization, along with quadrupolar broadening, makes the deuteron TE signal more difficult to measure with high accuracy. The cold NMR system can be used to improve the signal-to-noise ratio of the NMR signal [**?**].

The deuteron polarization can also be extracted from the shape of the NMR signal. The deuteron is a spin-1 nucleus with three magnetic substates, $m = -1, 0, +1$, and the NMR absorption signal lineshape is the sum of the two overlapping absorption lines consisting of the $-1 \rightarrow 0$ and $0 \rightarrow +1$ transitions. In the case of $^{14}ND_3$, the deuteron's electric quadrupole moment interacts with electric field gradients within the molecule and splits the degeneracy of the two transitions. The degree of splitting depends on the angle between the magn etic field and direction of the electric field gradient. The resultant linshape, integrated over a sample of many polycrystalline beads has the form of a Pake doublet. It has been experimentally demonstrated that, at or near steady-state conditions, the magnetic substates of deuterons in dynamically polarized $^{14}ND_3$ are populated according to the Boltzmann distribution with a characteristic spin temperature T that can be either positive or negative, depending on the sign of the polarization.

When the system is at thermal equilibrium with the solid lattice, the deuteron polarization is known from:

$$P_z = \frac{4 + \tanh \frac{\mu B}{2kT}}{3 + \tanh^2 \frac{\mu B}{2kT}} \tag{18}$$

where μ is the magnetic moment, and k is Boltzmann's constant. The vector polarization can be determined by comparing the enhanced signal with that of the TE signal (which has known polarization). This polarimetry method is typically reliable to about 5% relative.

Similarly, the tensor polarization is given by:

$$P_{zz} = \frac{4 + \tanh^2 \frac{\mu B}{2kT}}{3 + \tanh^2 \frac{\mu B}{2kT}} \tag{19}$$

From Eqs. 18 and 19, we find:

$$P_{zz} = 2 - \sqrt{4 - 3P_z^2} \tag{20}$$

In addition to the TE method, polarizations can be determined by analyzing NMR lineshapes as described in missing citation [**?**] with a typical 5-7% relative uncertainty. At high polarizations, the intensities of the two transitions differ, and the NMR signal shows an asymmetry R in the value of the two peaks. The vector polarization is then given by:

$$P_z = \frac{R^2 - 1}{R^2 + R + 1} \tag{21}$$

and the tensor polarization is given by:

$$P_{zz} = \frac{R^2 - 2R + 1}{R^2 + R + 1} \tag{22}$$

This measuring technique can be used as a compliment to the TE method resulting in reduced uncertainty in polarization for vector polarizations over 20%.

The measurement of the neutron polarization (P_n) is achieved by a calculation using the NMR measured polarization of the deuteron (P_d). The quantum mechanical calculation using Clebsch-Gordan coefficients show 75% of the neutron spins in the D-state are antiparallel to the deuteron spins [35]. The resulting neutron polarization is,

$$P_n = (1 - 1.5\alpha_D)P_d \approx 0.91P_d,$$

where α_D is the probability of the deuteron to be in a D-state.

7.2.3 Target Polarization Uncertainty

The lower limit for polarization uncertainty is set by the Q-meter style NMR which can not be expected to preform better that 1% relative error. UVA test lab studies have gone down as far as 1.5% but typically in an experiment 2-4% is achieved for the proton. The Deuteron/neutron has much larger error but with the use of the cold NMR system unknown citation [**?**] in combination with the multiple measurement techniques it is possible to reach the same uncertainty as for the proton measurement..

7.2.4 Active Target Contributions

The figure of merit for this type of polarized target experiment is proportional to the active target contribution squared times polarization squared. The active target contribution is made of of the dilution factor and the packing fraction over the length of the target. The packing fraction can be measured using a method of cryogenic volume displacement measurement which compare an empty target cell to the fill target cell used in the experiment. The target cell is filled with beads of solid NH3 material with a typical packing factor of about 50% with the rest of the space filled with liquid helium.

The dilution factor is the ratio of the number of polarizable nucleons to the total number of nucleons in the target material and can be defined as,

$$f = \frac{N_{D,H}\sigma_{D,H}}{N_N\sigma_N + N_{D,H}\sigma_{D,H} + \Sigma N_A\sigma_A}, \tag{23}$$

where N_D is the number of deuteron nuclei in the target and σ_D is the corresponding inclusive double differential scattering cross section, N_N is the nitrogen number of scattered nuclei with cross section σ_N, and N_A is the numbers of other scattering nuclei of mass number A with cross section σ_A. The denominator of the dilution factor can be written in terms of the relative volume ratio of ND_3 to LHe in the target cell, the packing fraction p_f. I am not sure I understand the following section: , our target is aligned orthognal to the fieldFor the case of a cylindrical target cell oriented along the magnetic field, the packing fraction is exactly equivalent to the percentage of the cell length filled with NH_3 or ND_3. The dilution factor for NH_3 is 0.176 and for ND_3 is 0.3. The uncertainty in these factors is typically 2-3%.

7.3 Luminosity and Beam Intensity

KL,DK

7.3.1 Beam Profile

The profile of beam delivered to the target is a two dimensional gaussian $\sigma_x = 6.8$ mm, $\sigma_y = 7.6$ mm. The beam will be cut off at 2.5σ, giving a beam profile of $\Delta x = 17$ mm, $\Delta y = 19$ mm (see left plot in Fig. 16). The beam is expecte to drive no more than $\pm = 2$ mm in each direction. The uncertainty on the change of the luminosity of the beam due to the beam drifting in x,y direction is

$$\Delta\mathcal{L}^2 = \frac{N_{gain}^2 + N_{lost}^2}{N_{beam}^2} \tag{24}$$

Figure 16 demonstrates that for a beam drift of $x_{drift} = 2$ mm. Using Eq. 24, there is an uncertainty in the Luminosity of $\Delta\mathcal{L} = 1.65\%$ for $x_{drift} = \pm 2$ mm, and$\Delta\mathcal{L} = 1.46\%$ for $y_{drift} = \pm 2$ mm.

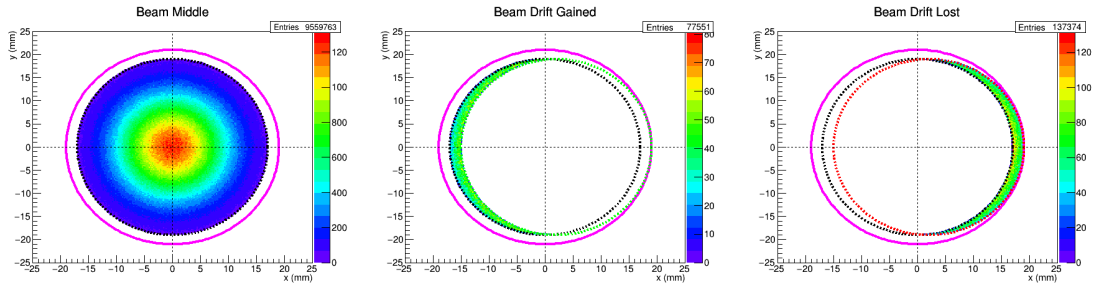

Figure 16: Fast Monte-Carlo Plot demonstrating the beam drift. Magenta curve represents the Target Area. The dashed ellipse represents the beam, with 2.5 sigma cut off due to swics. Left: Typical beam profile. Middle: Beam gained when the beam is off center $x = 2$ mm. Right: Beam lost when teh beam is off center $x = 2$ mm.

7.4 Geometrical Asymmetries

A further source of systematic uncertainty comes from the geometrical acceptance of the dimuon spectrometer. To get an estimate for systematic uncertainty in the A_N measurement as a result of the spectrometer, the existing E906 data was used.

Spin Change	σ_{stat}	RMS	σ_{sys}
every event	0.76%	0.76%	0.0%
8 hours	0.76%	0.85%	0.38%
12 hours	0.76%	0.94%	0.55%
24 hours	0.76%	0.11%	0.80%
48 hours	0.76%	0.13%	1.1%

Table 5: The systematic error from the SeaQuest spectrometer on A_N vs time between spin changes.

A high statistic, spectrometer stable part of the E906 was used for this check. With a cut on dimuons of $p_T > 0.5$ GeVc, and $0.2 < x_F < 0.7$, a total of $\sim$35K dimuons were analyzed. An up-down spin direction was assigned randomly after a given length of data, and A_N was calculated. This process is repeated 5000 times. With random assignment of the spin direction, a gaussian asymmetry distribution centered around zero is expected. The RMS of the gaussian should correspond to the statistical + systematic uncertainty, $RMS^2 = \sigma^2_{stat} + \sigma^2_{syst}$

The study was repeated five times, changing the length of data between spin assignments each time. An example of the gaussian distribution for changing the spin direction once a day is shown in Fig. 17. The results are summarized in table 5.

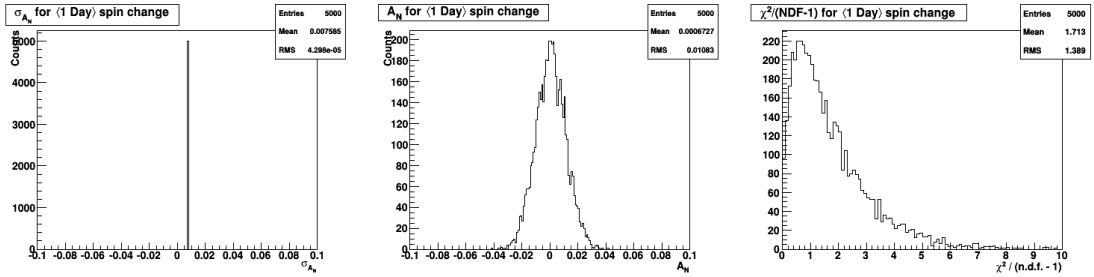

Figure 17: Plots describing the A_N of the E906 where spin direction is changes once a day. Left: The Mean value is the σ_{stat} on A_N. Middle: The distribution of A_N, where $RMS^2 = \sigma^2_{stat} + \sigma^2_{syst}$. Right: The reduced χ^2 of each extracted A_N value.

A closer look at Table 5 indicates that in an ideal world where we could reset the spin direction every event would give no systematic error. In reality, the target spin will be flipped anywhere from 8-24 hours. The current running plan is to

flip every 8 hours, which gives a total systematic on the A_N measurement from the spectrometer of $\sigma_{sys} = 0.38\%$. Worst case the spin would be flipped every 12 hours giving $\sigma_{sys} = 0.55\%$.

The results from this analysis are shown in Fig. **??** and show no geometrical asymmetry. To further reduce possible long term effects we plan to change the polarization of the target through change of the micro wave frequency every 8 hours. In addition, we will change the filed direction the polarized target magnet once during one target load as well as the direction of the field of the spectrometer. Combining measurements from different geometrical configuration with the same target cells will allow us to monitor for possible systematic drifts in the asymmetry.

In order to control systematic uncertainties from changing beam conditions, like position, luminosity and shape we will use several detectors and techniques. The absolute beam intensity will be determined by the Secondary Emission Monitors (SEM) which are upstream of the target. Their absolute precision has been established from the E906 data to be give number. We will use four detectors at 90 $\deg$ to the beam (two horizontally and two vertically) to help monitor the relative luminosity. These detectors will each consist of 4 plastic scintillators in coincidence and positioned outside of the shielding wall, pointing through a small hole in the shielding at the target. The ratio of every one of these detectors over the SEM will provide a relative luminosity measurement for each target spin configuration. As an additional check on the relative beam intensity we will use a four plate RF cavity, which can determine relative changes in the beam position to a precision of give a number. While online mesurements of the hodoscpope trigger road ratio for the left and right together with the luminosity counters will provide a beam movement indication, we will track this off line with single muon rates from the target.

Since extractting the Sivers asymmetry for the $d(\bar{x})$requires the measurement of ratio of the $\frac{\sigma^{pd}}{2\sigma^{pp}}$ care has to be taken that the running conditions for both targets are as identical as possible. Our target system will have two identical cells, one of them filled with NH_3 and the other with ND_3, which will be interchanged on a regular basis, thus minimizing systematic effects.

Finally, a carbon target will be used to measure zero asymmetry for every target stick configuration.

7.5 Overall Systematic Error

all

I think that for a ΔA of 2% statistical we should shoot for a 2-3% overall systematic error

In the following we will discuss the various sources of systematic errors and the plans to ameliorate them. We estimate that the major contribution will come from the measurement of the target polarization ($\approx 2-3$ %) and the determination of the dilution factor (≈ 3 %) as described above.

7.6 Expected Results

all

7.7 Comparison with other experiments

PLM, Ak et al

This table.....

8 Budget Discussion

In the following we will describe some of the major cost expenditures of experiment E1039 and the current estimates.

8.1 Liquefier System

The major cryogenic issues with a polarized 4He target are the liquid He consumption and the collection of the exhaust gas. Keeping the target at 1K will lead to a overall consumption of roughly 100 liters of liquid He per day. This is a sizable amount of a nonrenewable resource, as well as a large cost. Furthermore, such a system will need a special plumbing and recovery infrastructure consisting of Helium and Nitrogen transferlines, pumping lines from the target to the ROOTS pumps as well as a special quenchline, which would handle the Helium exhaust gas in case of a magnet quench. We have identified two liquefiers (one at FNAL and one at University of Illinois), which we could refurbish. Quantum Technology has provided us with a preliminary bid for a closed loop system, based on refurbishing one of these liquefiers at 550,000 $. This is based on a refurbishing cost

Experiment	Particles	Energy (GeV)	x_b or x_t	Luminosity ($cm^{-2}\,s^{-1}$)		P_b or P_t (f)	rFOM[#]
(COMPASS CERN)	$\pi^{\pm} + p^{\uparrow}$	160 GeV $\sqrt{s}$ = 17	$x_t = 0.2 - 0.3$	2×10^{33}	0.14	P_t = 90% f = 0.22	1.1×10^{-3}
PANDA (GSI)	$p + p^{\uparrow}$	15 GeV $\sqrt{s}$ = 5.5	$x_t = 0.2 - 0.4$	2×10^{32}	0.07	P_t = 90% f = 0.22	1.1×10^{-4}
PAX (GSI)	$p^{\uparrow} + p$	collider $\sqrt{s}$ = 14	$x_b = 0.1 - 0.9$	2×10^{30}	0.06	P_b = 90%	2.3×10^{-5}
NICA (JINR)	$p^{\uparrow} + p$	collider $\sqrt{s}$ = 26	$x_b = 0.1 - 0.8$	1×10^{31}	0.04	P_b = 70%	6.8×10^{-5}
PHENIX (RHIC)	$p^{\uparrow} + p$	collider $\sqrt{s}$ = 500	$x_b = 0.05 - 0.1$	2×10^{32}	0.06	P_b = 60%	3.6×10^{-4}
SeaQuest (FNAL: E-906)	$p + p$	120 GeV $\sqrt{s}$ = 15	$x_b = 0.35 - 0.9$ $x_t = 0.1 - 0.45$	3.4×10^{35}	---	---	---
Pol tgt DY[‡] (FNAL: E-1039)	$p + p^{\uparrow}$	120 GeV $\sqrt{s}$ = 15	$x_t = 0.1 - 0.45$	3.1×10^{35}	0 – 0.2*	P_t = 80% f = 0.176	0.09
Pol beam DY[§] (FNAL: E-1027)	$p^{\uparrow} + p$	120 GeV $\sqrt{s}$ = 15	$x_b = 0.35 - 0.9$	2×10^{35}	0.04	P_b = 60%	1

[‡] *8 cm NH_3 target* [§] *L= 1 x 10^{36} $cm^{-2}\,s^{-1}$ (LH_2 tgt limited) / L= 2 x 10^{35} $cm^{-2}\,s^{-1}$ (10% of MI beam limited)*
**not constrained by SIDIS data* / [#] rFOM = relative lumi * P^2 * f^2 wrt E-1027 (f=1 for pol p beams)

ak

Figure 18: *Comparison with planned experiments*

of 30,000 $. A firm estimate for the refurbishing can only be provided when the liquefier is at Quantum Technoloy and evaluetd for the refurbishing work needed. The costs for the Helium and Nitrogen transfer lines is estimated to be 50,000$. This will depend on the finalized placement of the liquefier system.

8.2 Beam Line Changes

Carol Johnstone

8.3 Shielding and Traget Cave modifications

This cost can only be estimated when the final design of the shielding has been performed. This will require close collaboration between ES&H, Accelerator and

Physics divisions at FNAL with LANL engineering. The main cost of this will be labor costs for restacking the shielding. The FNAL estimate for completely unstacking (which is more than we would need) the SeaQuest shielding is 40,000$.

9 Fermilab PAC 2013 and 2015 reviews and LANL Reviews

9.1 Fermilab PAC

In 2013 the measurement of the Sivers asymmetry was presented to the FNAL Program Advisory Committee (PAC) as a letter of intent (P-1027), which can be found in the appendix A.3. Even though we submitted this as a LOI, the PAC recommended stage-1 approval, a testimony to the quality of the physics. At Fermilab, the PAC can only approve stage-1, while stage-2 is granted by the director, once the funding for the experiment has been secured. In the following we quote the relevant section from the 2013 PAC report **??**:

Drell-Yan Experiment with a Polarized Proton Target (P-1039) *Members of the SeaQuest Collaboration presented a proposal (P-1039) for a new Drell-Yan experiment at Fermilab. P-1039 proposes to perform the first measurement of the Sivers function of sea anti-quarks by adding a new LANL-designed polarized proton target to the existing E906 detector. No major changes are required to the beam line. The physics addressed by P-1039 is similar to that addressed by P-1027, a proposal presented to the PAC in 2012. Both propose to perform measurements aiming to resolve the proton spin puzzle, a topic that is important to the nuclear physics community and is of interest to the high-energy physics community as well. While P-1027 aims to measure the Sivers function for valence quarks, P-1039 proposes to perform the same measurement on sea anti-quarks. Since there are indications from other experiments that the Sivers function for valence quarks is small, the measurement proposed by P-1039 is more promising in terms of providing a possible solution to the proton spin puzzle. By using a polarized target instead of a polarized beam, P-1039 would address this interesting physics topic while keeping to a minimum the impact on the Fermilab accelerator division and the rest of the Fermilab physics program. This is not the case for P-1027, which requires significant resources to develop a polarized beam and which*

more severely disrupts the beam to NOvA. The PAC also appreciates the opportunity offered by this proposal to continue the partnership between Fermilab and the nuclear physics community. Given the pressure on the accelerator division and the overriding responsibility of the Lab to support its core neutrino program, the PAC recommends that priority should be given to P-1039 over P-1027, and hence recommends Stage-1 approval for P-1039, contingent on the funding from DOE Office of Nuclear Physics (NP) for the project and continued minimal impact on the high-priority core program. Because of the significantly smaller impact of P-1039 on the Fermilab infrastructure, NP funding could be easier to obtain and the experiment could start earlier.

In Januray 2015 we presented an update to the PAC on the status of the preparation for the experiment, where again the PAC expressed their support for this effort **??**:

LOI: P-1039 UPDATE: Drell-Yan Experiment with Polarized Target (SeaQuest extension) *The SeaQuest extension E-1039 aims at resolving the proton spin puzzle, and in particular measuring the Sivers function for sea quarks. E-1039 is planned to achieve a sensitivity level far superior to other experiments. The collaboration presented a very detailed and very well thought out plan for the transition from SeaQuest to E-1039.* ***The case was successfully made that unique measurements could be made by E-1039 to complement those from experiments at other facilities, notably COMPASS at CERN*** *(bold added for emphasis). The PAC appreciates the opportunity offered by this proposal to continue the partnership between Fermilab and the nuclear physics community. We encourage the development of a TSW in preparation for Stage 2 approval, which will require an expectation of full funding from the DOE Office of Nuclear Physics.*

9.2 LANL reviews

During the course of the LDRD project the LDRD office required two reviews of the physics , technical efforts and progress both in the experimental as well as the theoretical aspects of the LDRD project. The review panels included external as well as internal members of the community. The review committee for the first one in 2013 was composed of: C. Keith, Jefferson Lab, S. Kuhn, Old Dominion University and J. Qiu, Brookhaven National Laborartory

as external members and C. Olinger, M. Brooks and B. Louis from LANL as internal. The second committee consisted of G. Dodge, Old Dominion University,

and L. Gamberg, Penn State University as well as A. Hayes-Sterbenz and M. Brooks from LANL. In both reviews the physics as well as the work have been consistently deemed as outstanding. In the following we show excerpts from the two reviews:

Quality : Outstanding (review Jan 2015) *The quark and gluon Sivers functions of a polarized proton describe the quantum correlations between its spin and the direction as well as the strength of confined orbital motion of quarks and gluons within it. They encode critical information on the confined structure and motion of quarks and gluons making up the proton's properties, such as the spin, and are fundamental properties of QCD dynamics. The predicted sign change of the Sivers functions measured in Semi-inclusive DIS to that measured in Drell-Yan processes is deeply rooted in the gauge property of QCD and the validity of QCD factorization. Owing to the color confinement - the defining property of QCD, meaning that we can't probe the proton's partonic structure without QCD factorization - developing the formalism to precisely connect the QCD dynamics to the measured cross sections of leptons and hadrons is an area of active research. The predicted sign change of Sivers functions has been recognized as the most important test of and challenge to our understanding of QCD dynamics. It attracted tremendous theoretical and experimental effort worldwide to find a way to confirm or disapprove this prediction. The Sivers functions have been extracted from Semi-inclusive DIS experiments, but they have not been extracted from any Drell-Yan experiment yet. Along with the proton-proton Drell-Yan experiment of this DR at Fermilab, the COMPASS experiment at CERN is pursuing Drell-Yan measurement in pion-proton collisions, while the RHIC Spin program at Brookhaven National Lab is trying to extract the Sivers functions from its Drell-Yan like W-physics program. All three experiments worldwide are critically important and complementary to each other due to the difference in beams and energy scales where the Sivers functions are probed. The proposed measurement of Sivers functions for anti-quarks by this DR cannot be replaced by any currently proposed experiments, and will lead to a fundamental advance of our knowledge in hadron physics and QCD dynamics far beyond the more than thirty-year effort in extracting the parton distribution functions.*

Overall Grade: Outstanding

Appendices

A Appendices

A.1 Deuteron Tensor Function b_1

A.2 Explore gluon TMD/Twist-3 trigluon correlation functions and QCD dynamics with heavy quarks

One important physics we would like to study is the heavy quark TSSA in the polaried p+p collisions. TSSAs have been recognied as a means to access parton distributions and QCD dynamics, both whtin initial-state hadrons and in the process of hadronizaton from partons. Large TSSAs up to $\sim 50\%$ were observed in light hadron productions in the region of $x = 0.1\ 0.5$ "valene quark" region (pions and Koans etc.) but very limited data are availabel for the heavy flavor particles. Furthermore, these observed large asymmetries are normally attributed to the valence quarks' Sivers and/or Collins effects. However, due to limitations in all previous and on-going experiments, very little precision data are availabe for the gluon sector in this large-x region despite gluons contribute significantly in this "valence region", the gluon distribution is comprable with valence d-quark and u-quak distributions, see Figure 19.

Due to the large amount of gluons inside the proton at high-x region, it is expected that heavy quark productions ($J\Psi$, and open charm $etc.$) in E1039 experiment are dominated by gluon-gluon interaction thus the heavy flavor transverse single spin asymmetry is sensitive to the tri-gluon correlation functions (aka gluon's TMD Sivers functions in the TMD framework) which are poorly constrained by current data. Furthermore, unlike the two twist-3 quark-gluon correlation functions (the socalled "non-derivative" and "derivative" terms) that can be combined into one form to explain the the light hadron TSSA, for the gluonic sector, the two corresponding twist-3 trigluon correlation functions can't be cobined into one simple form due to the difference in the hard scattrering parts of these two term. See Figure 20.

As a consequency, the charm and anti-charm hadron TSSAs may not to identical anc could yield two distinct experimental signatures! Figure 21 show how charm and anti-charm hadrons could have very distinct TSSAs due to the two distinct tri-gluon correlation functions discussed above.

Measurements of heavy flavor charm and anti-charm TSSAs in E1039 are of

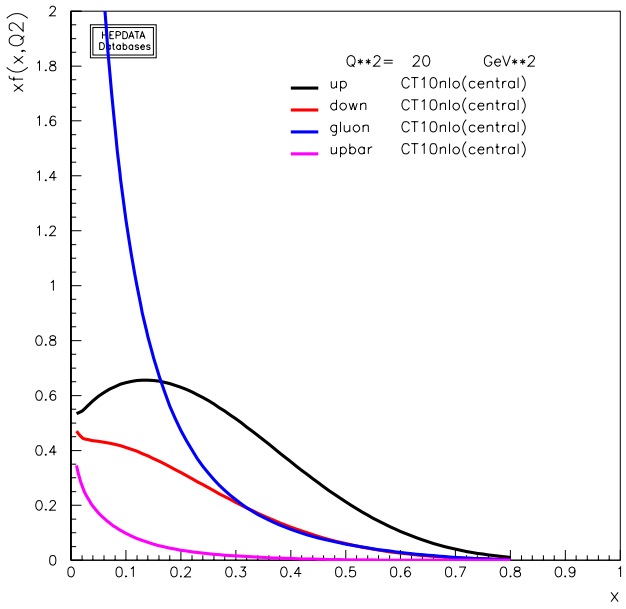

Figure 19: *Parton distributions vs x at* $Q^2 = 10GeV^2$*, from CT10. Note that there are significant amount of gluons in high-x region, comparable to the valence quarks.*

great interest becuase they can be used to isolate the two indepnendent trigluon distributions inside the polarized protons and the novel QCD dynamics in the high-energy polarized proton-proton collisions.

E1039 also privieds a unique opportunity to study fundamental pQCD approaches to particle prodcution in hadronic interactions. One good example is the NRQCD appraoch to $J\Psi$ produciton in hadronic interaction. Due to its high mass, it is expected that pQCD techinique can be applied to calculation of $J\Psi$ produci-

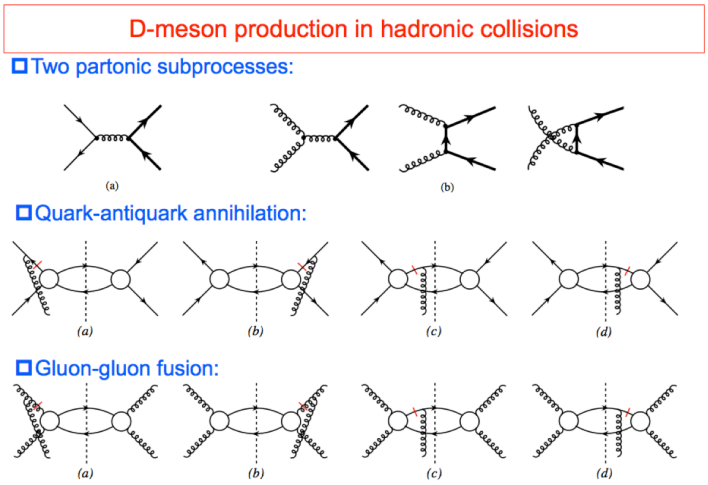

Figure 20: *Various processes contribute to the (anti)Charm TSSA in hadronic interaction. Top: at Leading-Order, charm and anticharm pairs are produced through quark and anti-quark fusion as well as gluon-gluon fusion processes. At E1039 energy, the gluonic processes dominate the production cross section; Middle: Feynman diagrams contribute to TSSA in the process of quark-anati-quark annailation into a pair of charm and anticharm; Bottom: Feynman diagrams contribute to TSSA in the gluon fusion process*

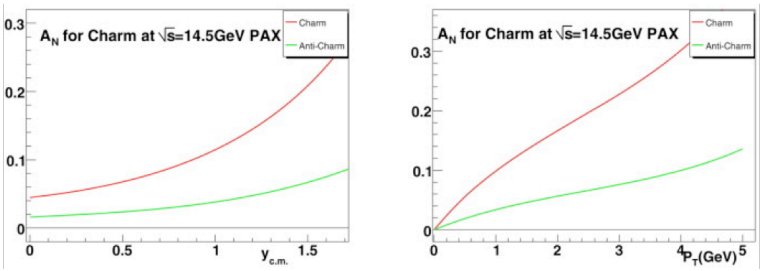

Figure 21: *Model calculations of expected Charm and anti-Charm hadron TSSAs in hadronic interaction. Left: Charm(Red) and antiCharm(Green) TSSAs vs rapidity y; Right:Charm(Red) and antiCharm(Green) TSSAs vs pT.*

ton in p+p collisions. It has been studeid over the last decades, but the details of the production mechanisms remain an open question and a major cahllenge for the application of pQCD. It is argued by Yuan [40]that within the framework of NRQCD and TMD factorization, the transveres single spin asymmetry of $J\Psi$ can be sensitive to the production channels, in particular, the color-octet and color-

singlet processes, assuming a non-zero gluon Sivers function. Specifically, Yuan showed that a nonzero gluon Sivers function will produce a finite TSSA for colro-singlet $J\Psi$ production channel in p+p collisions, but the asymmetry should valish for color-octet production process due to exact cancelation between initial and final state effects, see Figure 22. It should be noted that the relationship between the TSSA and the production mechanism is not quite sinple in the collinear twist-3 apparich, wiht only partial cancelation of terms in the case where the asymmetry uniforamly vanishes in the TMD approach presented by Yuna [41].

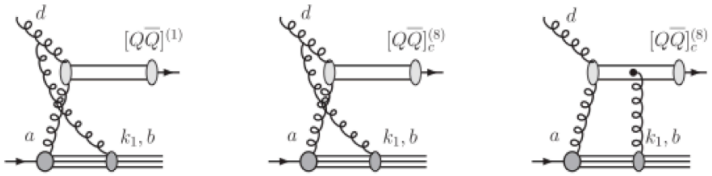

Figure 22: *Feynman diagrams contribute to$J\Psi$ TSSA in colore singlet (left) and colore-ocet (right 2) channels.*

Previous $J\Psi$ TSSA data from the PHENIX experiment at BNL suggest that gluon's Sivers functions are not large, however, the precision is very much statistically limited compared to light hadron asymmetry measurements.

A.3 Letter of Intent P-1039

.png 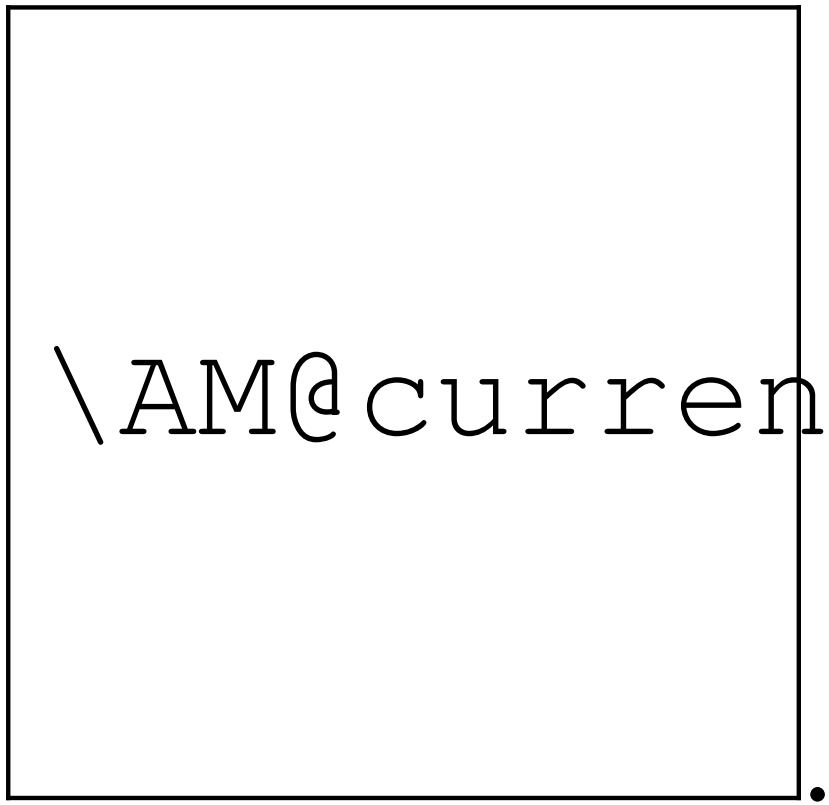 .png 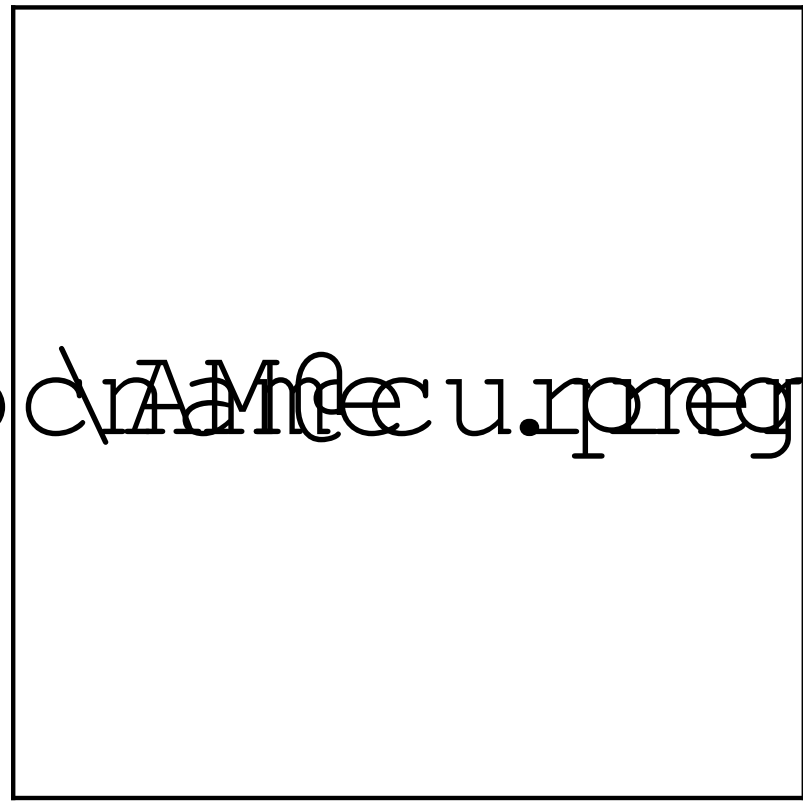

.png 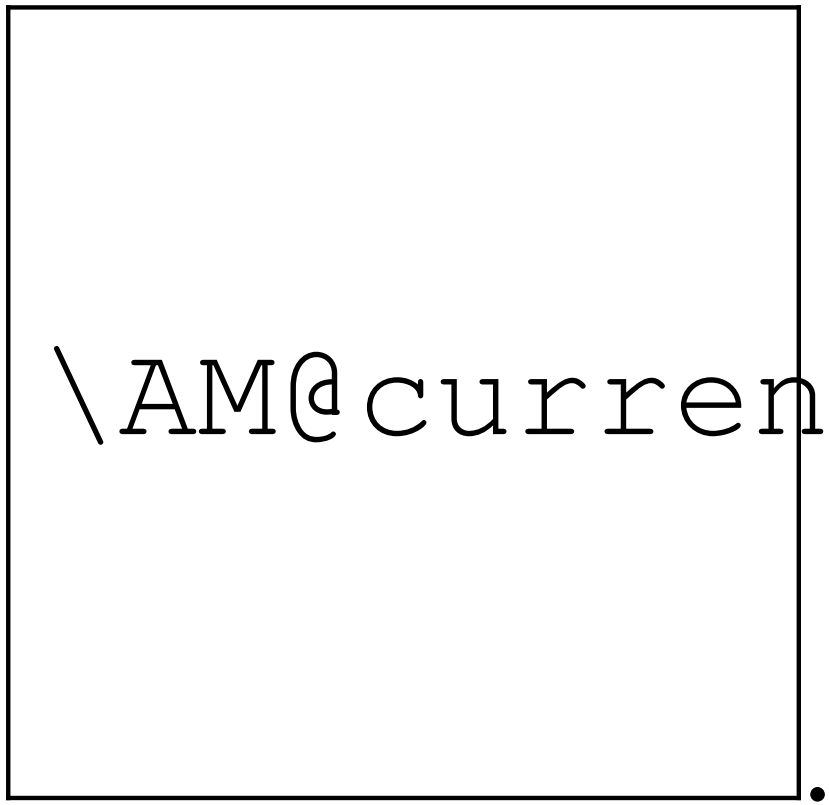 .png 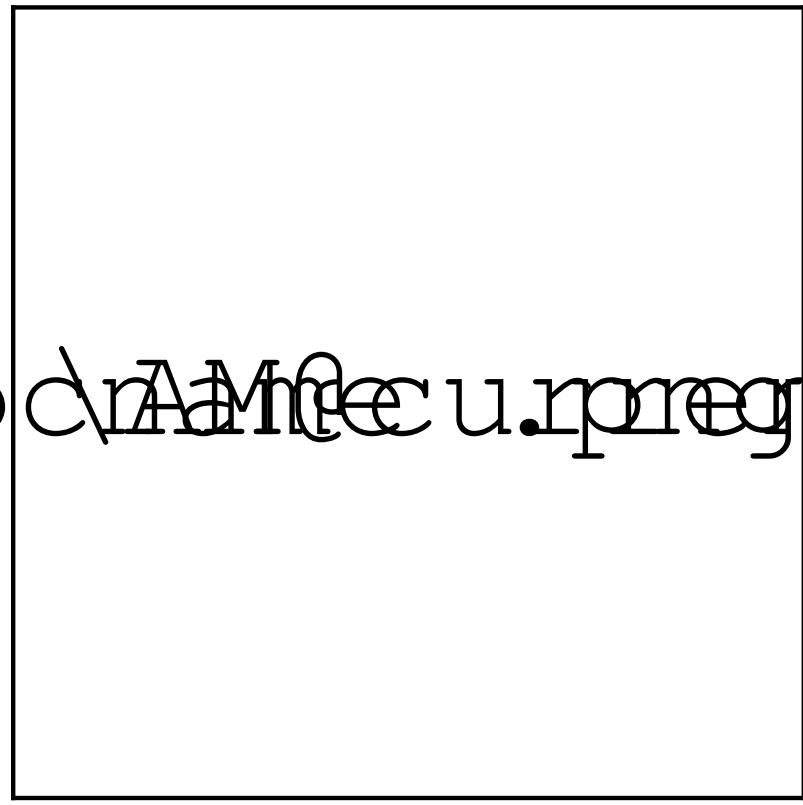

.png 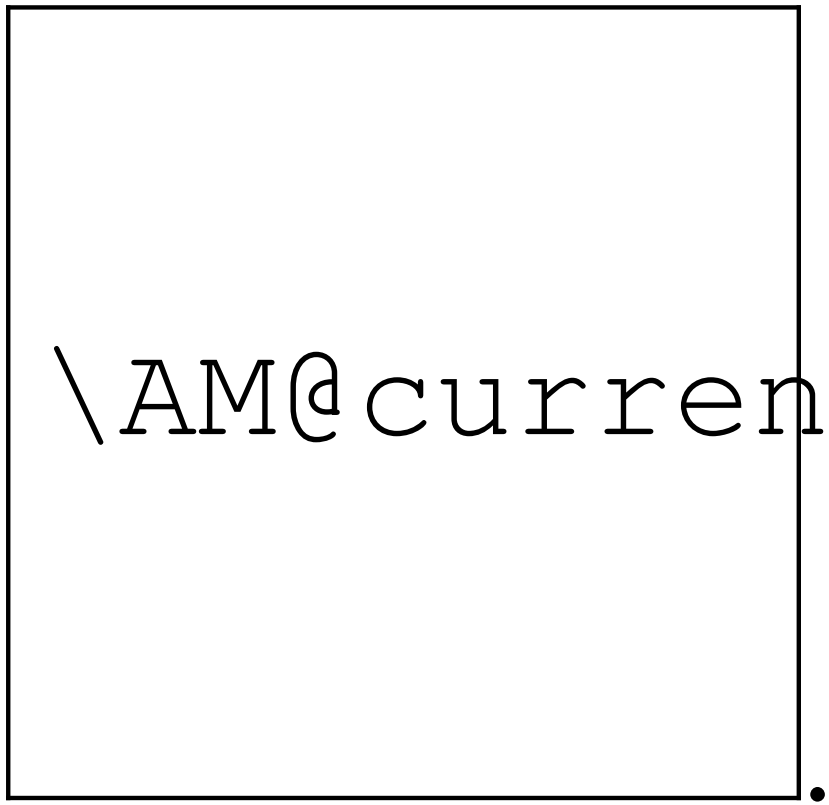 .png 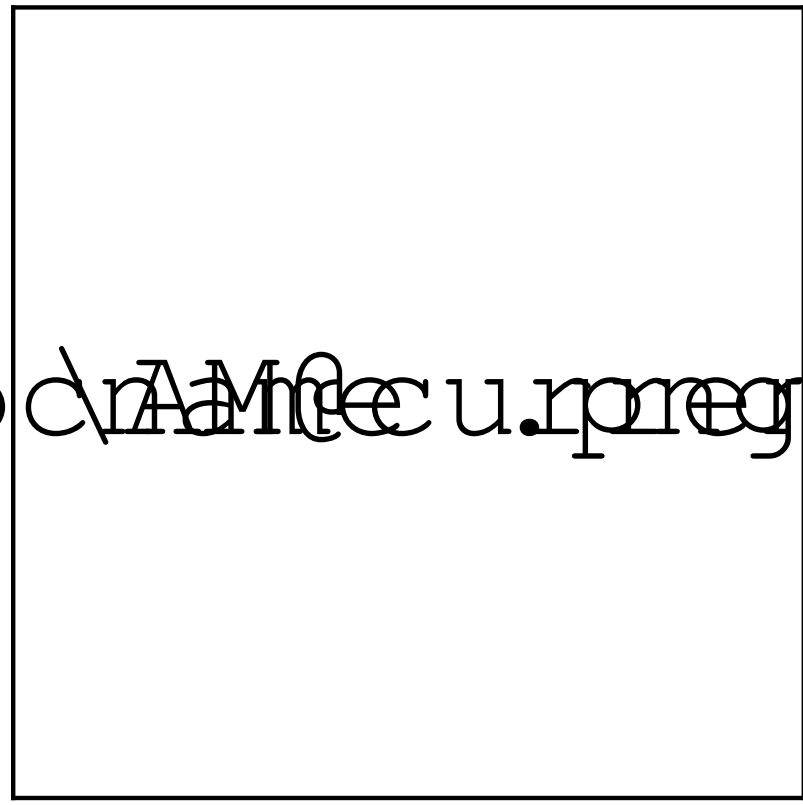

.png 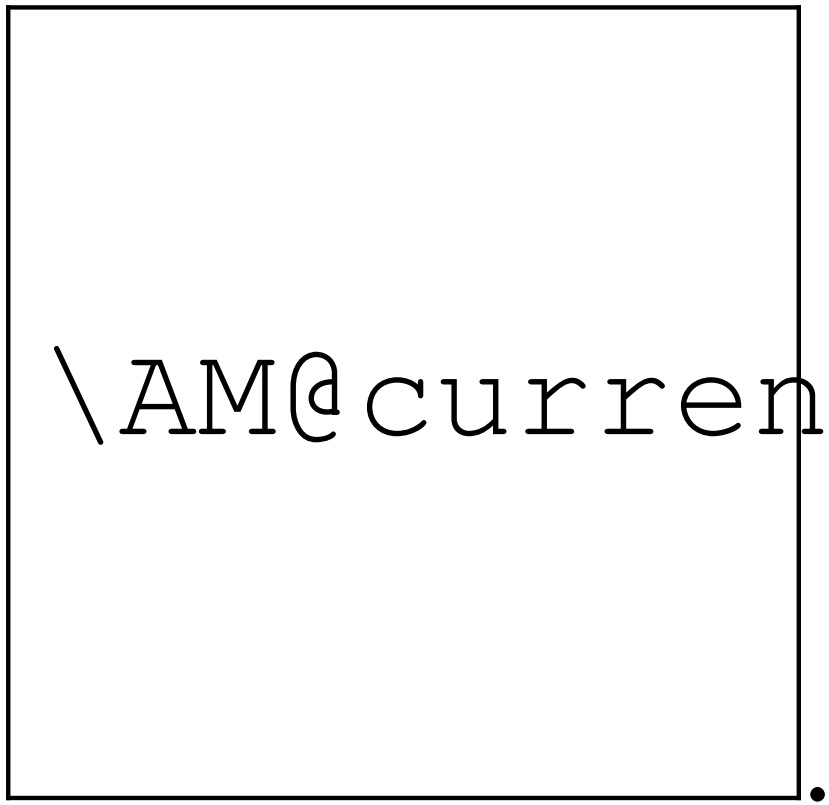 .png 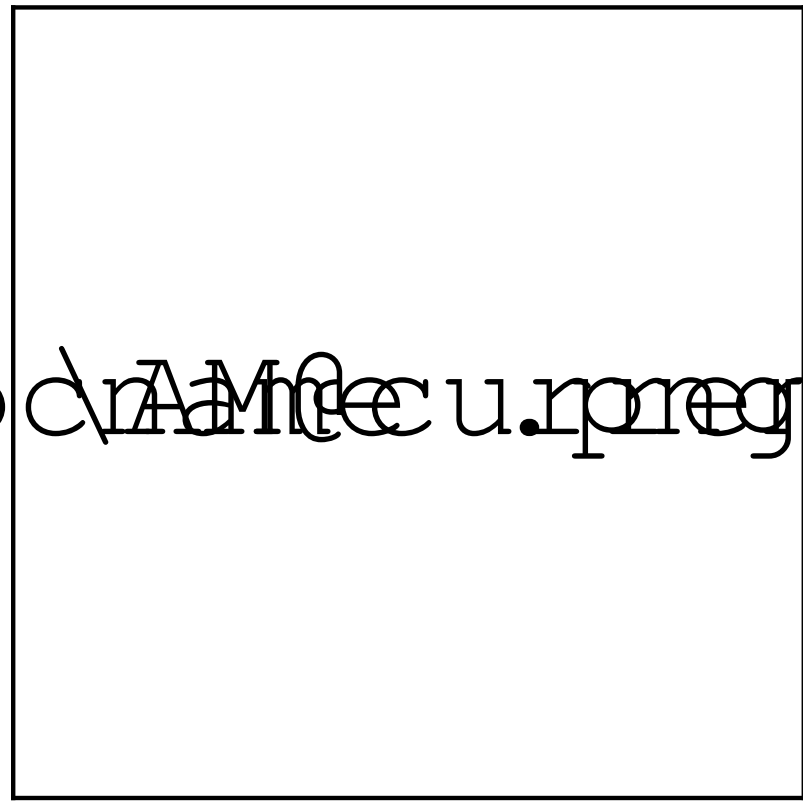

.png 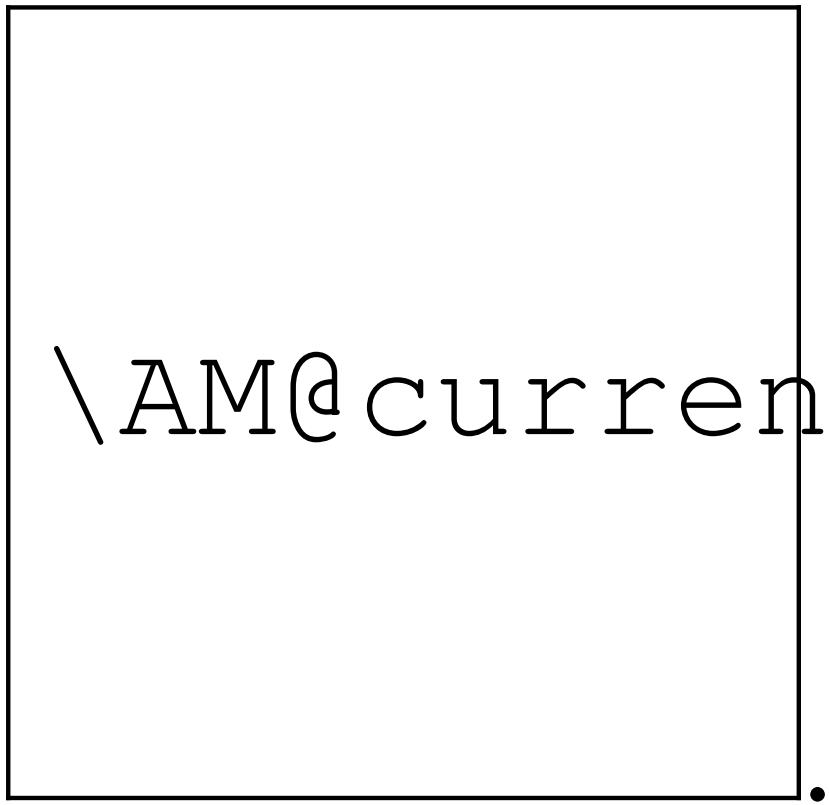 .png 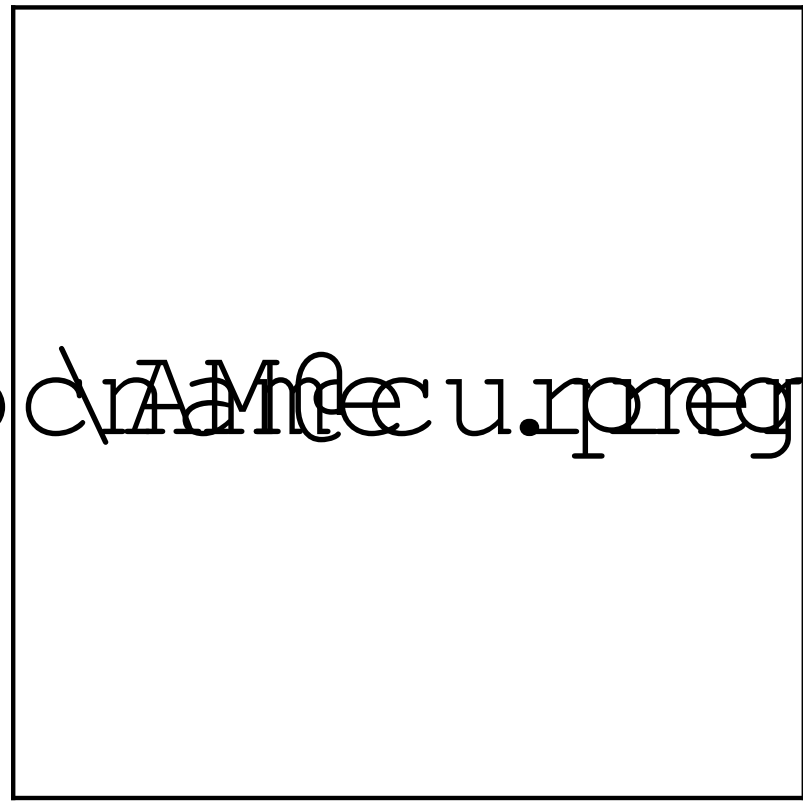

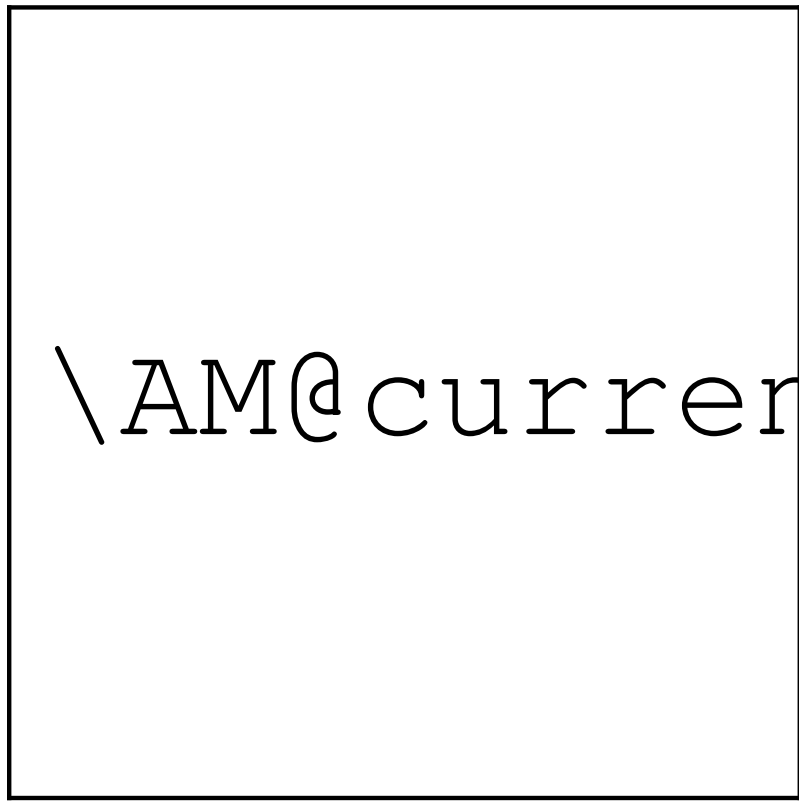

.png

A.4 LANL internal reviews

References

[1] D. Boer, M. Diehl, R. Milner, R. Venugopalan, W. Vogelsang, D. Kaplan, H. Montgomery and S. Vigdor et al., ?Gluons and the quark sea at high energies: Distributions, polarization, tomography?, arXiv:1108.1713 [nucl-th]

[2] A. Accardi, J. L. Albacete, M. Anselmino, N. Armesto, E. C. Aschenauer, A. Bacchetta, D. Boer and W. Brooks et al., ?Electron Ion Collider: The Next QCD Frontier - Understanding the glue that binds us all?, arXiv:1212.1701 [nucl-ex].

[3] E. Aschenauer, et al., ?The RHIC Spin Program: Achievements and Future Opportunities?, arXiv:1304.0079 [nucl-ex].

[4] D. Sivers, Phys. Rev. **D41** (1990) 83.

[5] D. L. Adams et al. [FNAL-E704 Collaboration], Phys. Lett. **B264** (1991) 462

[6] A. Airapetian et al. [HERMES Collaboration], Phys. Rev. Lett. **103** (2009) 152002

[7] M. Alekseev et al. [COMPASS Collaboration], Phys. Lett. **B673** (2009) 127

[8] X. Qian et al. [JLab Hall A Collaboration], Phys.Rev.Lett. **107** 2011 072003

[9] G. Garvey, Phys. Rev. **C81** (2010) 055212 and E866 collaboration, Phys. Rev. Lett. **80** (1998) 3715

[10] J. C. Collins, Phys. Lett. **B536** (2002) 43

[11] Fermilab E1027 proposal, 2012 http://ccd.fnal.gov/techpubs/fermilab-reports-proposal.html (FERMILAB-PROPOSAL-1027)

[12] SD . Drell and TM. Yan, Phys. Rev. Lett. **25** (1971) 316

[13] TMD Collaboration for the Coordinated Theoretical Approach to Transverse Momentum Dependent Hadron Structure in QCD, J.W. Qiu, W. Detmold, *et al.*, 2015

[10] J. C. Collins, Nucl. Phys. B **396**, 161 (1993)

[14] A. V. Belitsky, X. J and F. Yuan, Nucl. Phys. B 656 (2003) 165

[15] D. Boer, P. J. Mulders and F. Pijlman, Nucl. Phys. B **667**, 201 (2003)

[16] P. J. Mulders, PoS QCDEV **2015**, 005 (2015) [arXiv:1510.05871 [hep-ph]].

[17] M. G. Echevarria, A. Idilbi, Z. B. Kang and I. Vitev, Phys. Rev. D **89**, 074013 (2014)

[18] Collins, John C. and Soper, Davison E., Nucl. Phys. B **193**, 391 (1981)

[19] Ji, Xiang-dong and Ma, Jian-ping and Yuan, Feng, Phys. Rev. D **71**, 034005 (2005)

[20] Collins, John, Foundations of Perturbative QCD, Cambridge, UK: Univ. Pr. (2011)

[21] Becher, Thomas and Neubert, Matthias, Eur. Phys. J. C **71**, 1665 (2011)

[22] Echevarria, Miguel G. and Idilbi, Ahmad and Scimemi, Ignazio, JHEP **1207**, 002 (2012)

[23] Chiu, Jui-Yu and Jain, Ambar and Neill, Duff and Rothstein, Ira Z., JHEP **1205**, 084 (2012)

[24] Ji, Xiangdong and Sun, Peng and Xiong, Xiaonu and Yuan, Feng, Phys. Rev. D **91**, 074009 (2015)

[25] Aidala, C.A. and Field, B. and Gamberg, L.P. and Rogers, T.C., Phys. Rev. D **89**, 094002 (2014)

[26] Kang, Zhong-Bo and Xiao, Bo-Wen and Yuan, Feng, Phys. Rev. Lett. **107**, 152002 (2011)

[27] Sun, Peng and Yuan, Feng, Phys. Rev. D **88**, 114012 (2013)

[28] Leader, Elliot and Lorcé, Cédric, Phys. Rept. **541**, 163-248 (2014)

[29] Ji, Xiang-Dong, Phys. Rev. Lett. **78**, 610-613 (1997)

[30] K. F. Liu *et al.*, PoS LATTICE **2011**, 164 (2011)

[31] G. R. Court, et al., NIM **A 324** (1993) 433

[32] D, Crabb, NIM in Phys. Res. **A356** (1995) 9

[33] D. Keller, NIM **A 728** (2013) 133-144

[34] G. R. Court et al NIM in Phys. Res.,**A527** (2004) 253

[35] Kadansky V. "Photoproduktion negativer Pionen an einem polarisierten Neutronentarget", PhD. thesis. University of Bonn. BONN-IR-75-54 (1975)

[36] O. E. Krivosheev and N. V. Mokhov, A new MARS and its applications', Fermilab-Conf-98/043 (1998) and SARE3 KEK Proceedings 97-5 (1997)

[37] G. R. Court , et al. Nucl. Instr. & Meth. **A324** (1993) 433

[38] `http://pac.fnal.gov/meetings/` Recommendations 2013

[39] `http://pac.fnal.gov/meetings/` Recommendations 2015

[40] F. Yuan, Phys. Rev. D **78**, 014024 (2008)

[41] Z.-B. Kang, Private communications. (2016)